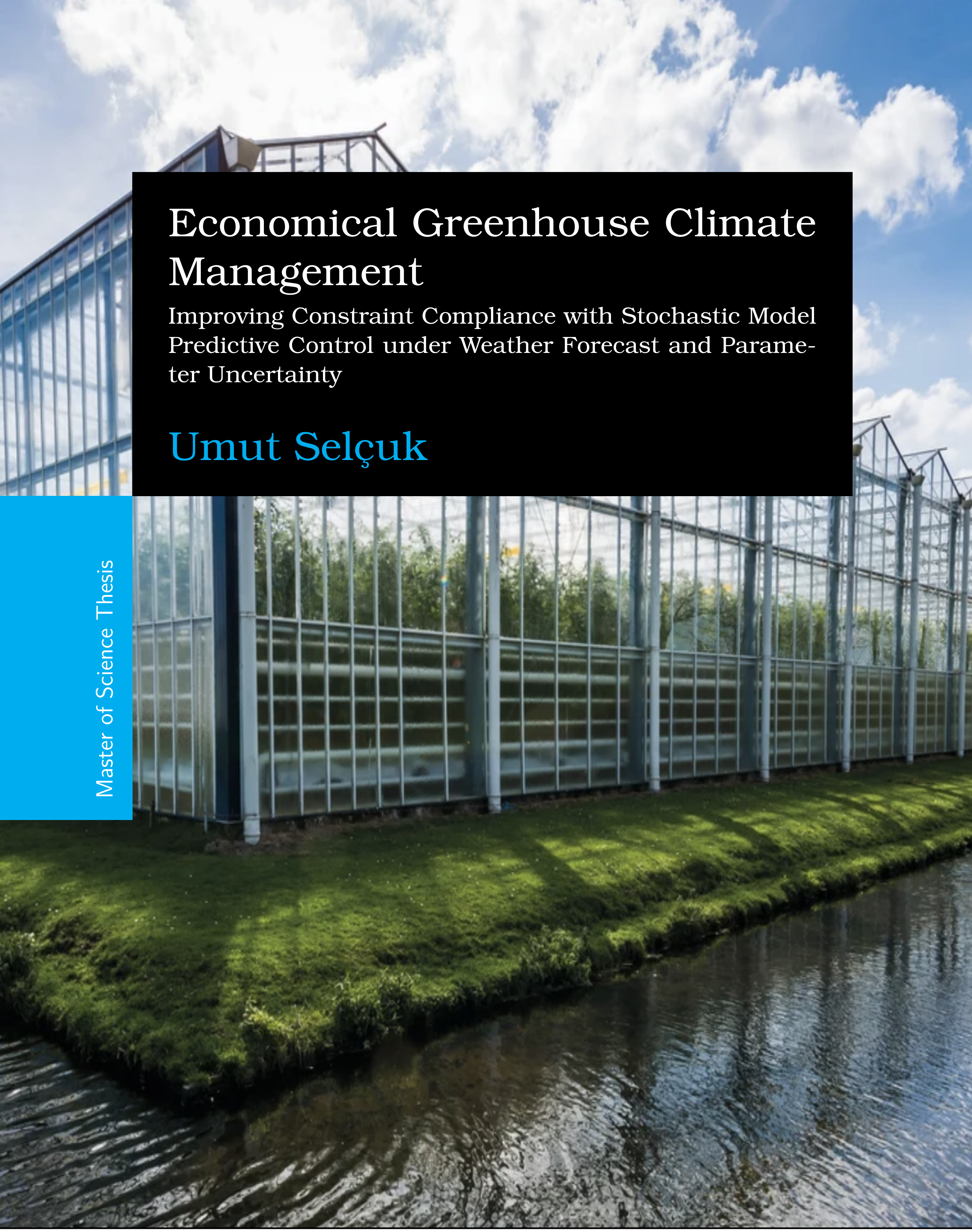

Economical Greenhouse Climate Management

Improving Constraint Compliance with Stochastic Model Predictive Control under Weather Forecast and Parameter Uncertainty

Umut Selçuk

Master of Science Thesis

Delft University of Technology

Delft Center for Systems and Control

Economical Greenhouse Climate Management

Improving Constraint Compliance with Stochastic Model Predictive Control under Weather Forecast and Parameter Uncertainty

Master of Science Thesis

For the degree of Master of Science in Systems and Control at Delft University of Technology

Umut Selçuk

April 20, 2025

Faculty of Mechanical Engineering (ME) · Delft University of Technology

Abstract

Several stochastic model predictive control schemes are formulated to reduce constraint violations in the economic control of the climate in a lettuce greenhouse under weather forecast and parameter uncertainty. The schemes are tested in simulation. Two separate approaches are taken in the formulations. The first involves analytical constraint tightening through system linearization. Linearizing the system around the trajectory is found to improve performance compared to linearizing around a point. The linearized schemes proved to be overly conservative, especially under parameter uncertainty. The second approach is through tracking the average constraint violations to formulate adaptive constraints which do not require prior information about the underlying uncertainties. Originally proposed for linear systems [31], this approach is simplified and modified to impose a constraint tightening on deterministic nonlinear model predictive control. The adaptive schemes improve constraint compliance with reduced conservatism leading to a more acceptable increase in input costs compared to the linearized schemes. The results indicate that adaptive average violation constraints may be a useful tool in stochastic model predictive control and warrant further investigation.

Table of Contents

Acknowledgements

First and foremost, I would like to thank my supervisor Dr. Robert (Koty) McAllister. I benefited greatly from his warm guidance and keen insight into the subject matter during my time working on this thesis.

Next, I would like to thank my classmates. I am grateful to have studied beside them, to have learned from them and to have enjoyed their company. I would also like to thank all the friends I made along the way who have made me feel fortunate calling Delft home for the past few years.

I would like to thank everyone who played a part in my journey and are dear to my heart. It pains me not to name each and every one of you. Finally, I want to thank my mother Ayten and my aunt Zehra. To them, I owe a debt I can never repay.

Delft, University of Technology
April 20, 2025

Umut Selçuk

“All knowledge degenerates into probability; and this probability is greater or less, according to our experience of the veracity or deceitfulness of our understanding, and according to the simplicity or intricacy of the question.”

— *David Hume*

Chapter 1

Introduction

Historically, the greenhouse provided extended growing seasons, shelter from adverse weather conditions and enabled the cultivation of exotic crops in regions that would otherwise be unfit. Currently, advanced greenhouses are equipped with systems that provide more precise control over the internal environment. This improved control allows experienced growers to achieve better quality and higher crop yields. In addition, farming in a controlled environment requires less use of pesticides, which can lead to a reduction in environmental pollution and less contaminants in produce. These advantages over open field farming come at a high initial investment cost and ongoing operational and maintenance costs. Despite these additional costs, advanced greenhouses are rapidly becoming more widespread due to their utility and efficiency, and are here to stay as a significant component of modern agriculture [4].

Until recently, greenhouse climate control systems relied primarily on multiple PID controllers [3] for set-point tracking, whereby an expert responsible for long-term planning determines the desired conditions inside, such as the humidity and temperature that the control system realizes. These may also be set to be dependent on the conditions, for example, the heaters can be turned down in sunny weather. This control structure is very practical as it provides the grower a lot of control over the environment without too many additional complications. However, it leaves much to be desired in terms of optimality, as it makes little use of the scientific knowledge about greenhouse dynamics in the short-term control and is entirely dependent on the capabilities of the expert for the long-term planning. The industrialization of the greenhouse, advances in optimal control theory, the development of accurate plant growth models, the availability of accurate weather forecasts and the increase in computing power enabled an optimal control approach to greenhouse climate control.

The optimal control approach utilizes theoretical models, sensor data and weather forecasts to predict the future behaviour of the greenhouse environment. Both short and long-term planning can then achieved by solving an optimization problem to find the control inputs that minimize an appropriate cost function. When the planning is formulated as such, the controller is also able to handle performance and control constraints. Such a solution can exploit predictions to save on costs while maintaining a safe environment that promotes plant growth. Implementing this type of optimization can result in more sustainable greenhouses and significant economic gains. It is crucial for these tools to be made demonstrably safe and beneficial, and accessible to the grower in order to see widespread adoption [64].

Recently, optimal control started seeing use in greenhouses in the model predictive control (MPC) framework [8][26], mostly for short-term (seconds, minutes) reference tracking. A separate long-term (hours, days) optimization is usually applied beforehand to generate the desired set points. This type of optimization considers longer timescales and often ignores transient dynamics. Incorporating the long-term optimization into the MPC controller can therefore lead to better performance, as such a controller would be able to better react to quick changes in conditions. This approach comes with its own shortcomings. A shortcoming of a traditional MPC controller is its inability to take into account uncertainties, which are always present due to errors in the model and disturbances. As optimal solutions often lie on some constraints, uncertainties often lead to constraint violations. This can be mitigated by setting conservative constraints and sacrificing optimality. Another approach, known as stochastic model predictive control (SMPC) [42], introduces uncertainties into the model and replaces the constraints with chance constraints that allow a certain probability of violation. This approach aims to improve constraint compliance while maintaining a balance between performance and robustness in the face of uncertainties.

SMPC results in a difficult and often infeasible optimization problem for nonlinear systems. Linearizing the greenhouse system, on the other hand, can lead to inaccurate predictions exacerbated by the difference in time scales between the fast greenhouse climate dynamics and the slow plant growth dynamics. A strategy to make the linearization more accurate is to solve the deterministic nonlinear problem and to use the resulting trajectory to obtain linearization points for the SMPC. An alternative strategy is to avoid linearization alltogether and instead use a constraint tightening formulation that can adapt to observed violations. Through these strategies, this thesis aims to develop and evaluate the efficacy of various SMPC controllers for economically optimal greenhouse climate management. By integrating chance constraints or adaptive constraints, the objective is to demonstrate more reliable constraint compliance compared to a corresponding deterministic MPC controller, while minimizing the extra costs incurred.

1-1 Research Goals and Thesis Outline

The research questions for this thesis are twofold:

- How can MPC be formulated for the economic optimization of climate control in a lettuce greenhouse with nonlinear dynamics while ensuring plant safety under uncertain **weather forecasts**? How does such a controller perform compared to nonlinear MPC in terms of cost and constraint satisfaction?
- How can MPC be formulated for the economic optimization of climate control in a lettuce greenhouse with nonlinear dynamics while ensuring plant safety under uncertain **model parameters**? How does such a controller perform compared to nonlinear MPC in terms of cost and constraint satisfaction?

Chapter 2 provides a summary of the relevant literature. Section 2-1 briefly describes the development of greenhouse climate and plant growth models and introduces the lettuce greenhouse model used in this study. Section 2-2 explains MPC and Section 2-3 goes over the literature on robust and stochastic MPC and some of their applications. Chapter 3 describes the specific control problem in detail together with the nature of the uncertainties that are considered. Chapter 4 introduces some analytical SMPC schemes obtained through stochastic constraints that exploit system linearization. Chapter 5 introduces an SMPC scheme with adaptive constraints. The simulation results and a discussion on the findings on the control schemes are presented in Chapter 6, and Chapter 7 contains the conclusions of this thesis.

1-2 Main Contributions

The main contributions of this thesis are the formulation of several stochastic model predictive control schemes for climate control in a lettuce greenhouse and their testing in simulation under weather forecast or parameter uncertainty. Two separate approaches were taken during the formulation of the schemes. Three schemes were constructed analytically through system linearization, linearizing the system around a trajectory instead of a point is shown to lead to lower constraint violations and cost in simulation. The remaining schemes were inspired by average violation constraints which were initially introduced for linear systems [31]. The formulation was simplified and modified to act as adaptive constraints for a nonlinear system. The adaptive schemes lead to comparable and potentially preferable results to the analytical schemes in simulation.

Chapter 2

Literature Survey

2-1 Greenhouse Dynamics

2-1-1 Greenhouse Models

The optimal control of the greenhouse depends on accurate models describing the dynamics involved the greenhouse climate and in plant growth. Work on such models for the purpose of control date back close to when computers were first introduced to the greenhouse [58]. Following Selçuk et al.[55], Kimball [30] simulated the steady-state thermal energy and vapour balances in a greenhouse and compared the simulation to experiments with promising results. The greenhouse was modeled as one-dimensional in the vertical direction, which is a widely used assumption effectively considering a section of a flat and horizontally uniform greenhouse of infinite area making the model easily scalable.

Building on steady state balances, Bot [10] introduced a dynamic model for a greenhouse climate using first-order differential equations and bond graphs for visual representation and simulation. It includes ventilation through openings by wind and thermal effects, short-wave and long-wave radiation (responsible for photosynthesis and radiative heating respectively) and their interplay with the greenhouse cover, transpiration and vapour pressure, and the thermal exchanges between the inside air, the outside environment, the greenhouse construction, layers of soil, the vegetation and the heating system. The model includes many simplifications, such as time-averaging fluctuating winds, and assuming uniform temperatures and humidities in the various components. Parts of the model were independently compared with results from corresponding experiments and the model parameters were adjusted to better match the experiments. The simulation of the complete model was demonstrated to reasonably approximate experimental results despite the simplifying assumptions.

Van Henten [60] constructed one of the earliest comprehensive dynamic models for a greenhouse combining greenhouse climate dynamics with crop growth dynamics for lettuce based on the research of Sweeney et al.[57]. The model, given below and illustrated in Figure 2-1, is derived from the literature ultimately relying on first principles and empirical studies, and expressed in ordinary differential equations in state-space. Explicitly put together for use in optimal control, it is more convenient compared to the Bot's model. The choice of lettuce as the crop also helps as it has simpler physiology compared to fruiting plants like the tomato which require separate models for different parts of the plant and different stages of their developments, e.g. the amount formed and the growth of leaves and fruits [28][19]. The simplest version of the greenhouse model given in Equation 2-1 consists of only four states: the dry-weight of the lettuce, the carbon dioxide concentration, the temperature and the humidity. All of the states are assumed to be uniform in space, i.e. all of the mass of the plant contributes evenly to all its processes and the air inside the greenhouse exhibits the same properties throughout. Carbon dioxide concentration, which is often omitted for short-term climate control, becomes an important factor when long-term plant growth is considered due to its effect on photosynthesis. The model considers the ventilation, heating and carbon dioxide injection as inputs which have a direct and instantaneous effect on the states. Their dynamics are left out which makes the model more general. In practice, those dynamics are to be either included or accounted for by lower level controllers. The effect of the environment is considered as exogenous inputs or disturbances, namely: the outside temperature, humidity and carbon dioxide concentration, and the incident radiation. The variables of the model are defined in Table 2-1.

$$
\begin{aligned}
\begin{bmatrix} \frac{\mathrm{d}x_{\mathrm{dw}}(t)}{\mathrm{d}t} \\ \frac{\mathrm{d}x_{\mathrm{CO_2}}(t)}{\mathrm{d}t} \\ \frac{\mathrm{d}x_{\mathrm{temp}}(t)}{\mathrm{d}t} \\ \frac{\mathrm{d}x_{\mathrm{hum}}(t)}{\mathrm{d}t} \end{bmatrix} &= \underbrace{\begin{bmatrix} c_{1,1}\phi_{\mathrm{phot}}(t) - c_{1,2}x_{\mathrm{dw}}(t)2^{(x_{\mathrm{temp}}(t)-25)/10} \\ \frac{1}{c_{2,1}}\left(-\phi_{\mathrm{phot}}(t) + c_{2,2}x_{\mathrm{dw}}(t)2^{(x_{\mathrm{temp}}(t)-25)/10} + u_{\mathrm{CO_2}}(t)10^{-6} - \phi_{\mathrm{vent,c}}(t)\right) \\ \frac{1}{c_{3,1}}\left(u_{\mathrm{heat}}(t) - (c_{3,2}u_{\mathrm{vent}}(t)10^{-3} + c_{3,3})(x_{\mathrm{temp}}(t) - d_{\mathrm{temp}}(t)) + c_{3,4}d_{\mathrm{rad}}(t)\right) \\ \frac{1}{c_{4,1}}(\phi_{\mathrm{transp}}(t) - \phi_{\mathrm{vent,h}}(t)) \end{bmatrix}}_{f(x(t),u(t),d(t),p)} \\
\phi_{\mathrm{phot}}(t) &= \left(1 - e^{-c_{1,3}x_{\mathrm{dw}}(t)}\right)\frac{c_{1,4}d_{\mathrm{rad}}(t)(-c_{1,5}x_{\mathrm{temp}}(t)^2 + c_{1,6}x_{\mathrm{temp}}(t) - c_{1,7})(x_{\mathrm{CO_2}}(t) - c_{1,8})}{c_{1,4}d_{\mathrm{rad}}(t) + (-c_{1,5}x_{\mathrm{temp}}(t)^2 + c_{1,6}x_{\mathrm{temp}}(t) - c_{1,7})(x_{\mathrm{CO_2}}(t) - c_{1,8})} \\
\phi_{\mathrm{vent,c}}(t) &= (u_{\mathrm{vent}}(t)10^{-3} + c_{2,3})(x_{\mathrm{CO_2}}(t) - d_{\mathrm{CO_2}}(t)) \\
\phi_{\mathrm{vent,h}}(t) &= (u_{\mathrm{vent}}(t)10^{-3} + c_{2,3})(x_{\mathrm{hum}}(t) - d_{\mathrm{hum}}(t)) \\
\phi_{\mathrm{transp}}(t) &= c_{4,2}\left(1 - e^{-c_{1,3}x_{\mathrm{dw}}(t)}\right)\left(\frac{c_{4,3}}{c_{4,4}(x_{\mathrm{temp}}(t) + c_{4,5})}\exp\left(\frac{c_{4,6}x_{\mathrm{temp}}(t)}{x_{\mathrm{temp}}(t) + c_{4,7}}\right) - x_{\mathrm{hum}}(t)\right) \\
\begin{bmatrix} y_{\mathrm{dw}}(t) \\ y_{\mathrm{CO_2}}(t) \\ y_{\mathrm{temp}}(t) \\ y_{\mathrm{hum}}(t) \end{bmatrix} &= \underbrace{\begin{bmatrix} 10^3 x_{\mathrm{dw}}(t) \\ \frac{10^2 c_{2,4}(x_{\mathrm{temp}}(t) - c_{2,5})}{c_{2,6}c_{2,7}}x_{\mathrm{CO_2}}(t) \\ x_{\mathrm{temp}}(t) \\ \frac{10^2 c_{2,4}(x_{\mathrm{temp}}(t) - c_{2,5})}{11\exp\left(\frac{c_{4,6}x_{\mathrm{temp}}(t)}{x_{\mathrm{temp}}(t)+c_{4,7}}\right)}x_{\mathrm{hum}}(t) \end{bmatrix}}_{g(x(t),p)}
\end{aligned}
\tag{2-1}
$$

The dynamics included in the model which affect plant growth are photosynthesis and respiration, both of which also affect the carbon dioxide concentration. The transpiration of the lettuce is considered in the humidity. Similar to heat, humidity and carbon dioxide are ex-

Table 2-1: Meaning of the states $x(t)$, inputs $u(t)$, outputs $y(t)$ and disturbances $d(t)$.

$x_{\mathrm{dw}}(t)$	Dry-weight (kg/m^2)	$y_{\mathrm{dw}}(t)$	Dry-weight (g/m^2)
$x_{\mathrm{CO_2}}(t)$	Indoor CO_2 (kg/m^3)	$y_{\mathrm{CO_2}}(t)$	Indoor CO_2 (ppm)
$x_{\mathrm{temp}}(t)$	Indoor temperature (°C)	$y_{\mathrm{temp}}(t)$	Indoor temperature (°C)
$x_{\mathrm{hum}}(t)$	Indoor humidity (kg/m^3)	$y_{\mathrm{hum}}(t)$	Indoor humidity (%)
		$d_{\mathrm{rad}}(t)$	Irradiation (W/m^2)
$u_{\mathrm{CO_2}}(t)$	CO_2 injection (mg/m^{2}s)	$d_{\mathrm{CO_2}}(t)$	Outdoor CO_2 (kg/m^3)
$u_{\mathrm{heat}}(t)$	Heating (W/m^2)	$d_{\mathrm{temp}}(t)$	Outdoor temperature (°C)
$u_{\mathrm{vent}}(t)$	Ventilation (mm/s)	$d_{\mathrm{hum}}(t)$	Outdoor humidity (kg/m^3)

changed with the environment due to diffusion and natural ventilation at a rate proportional to the difference in concentrations, this can be accelerated with the ventilation input. The temperature and the carbon dioxide concentration can be directly controlled with the heating and carbon dioxide injection inputs respectively. Finally, solar irradiation increases the temperature and is required for photosynthesis. The constant parameters are derived from the literature or from experiments. They are useful in simplifying the model, such as providing an aggregate heat transfer constant to account for all conduction and convection effects. Simulations of the model were demonstrated to match experiments with reasonable accuracy [61] and the parameters used are given in Table 2-2. The model is compact and straightforward while still incorporating the dynamics which are most impactful for economically optimal greenhouse climate control. This makes it ideal for the purposes of this thesis.

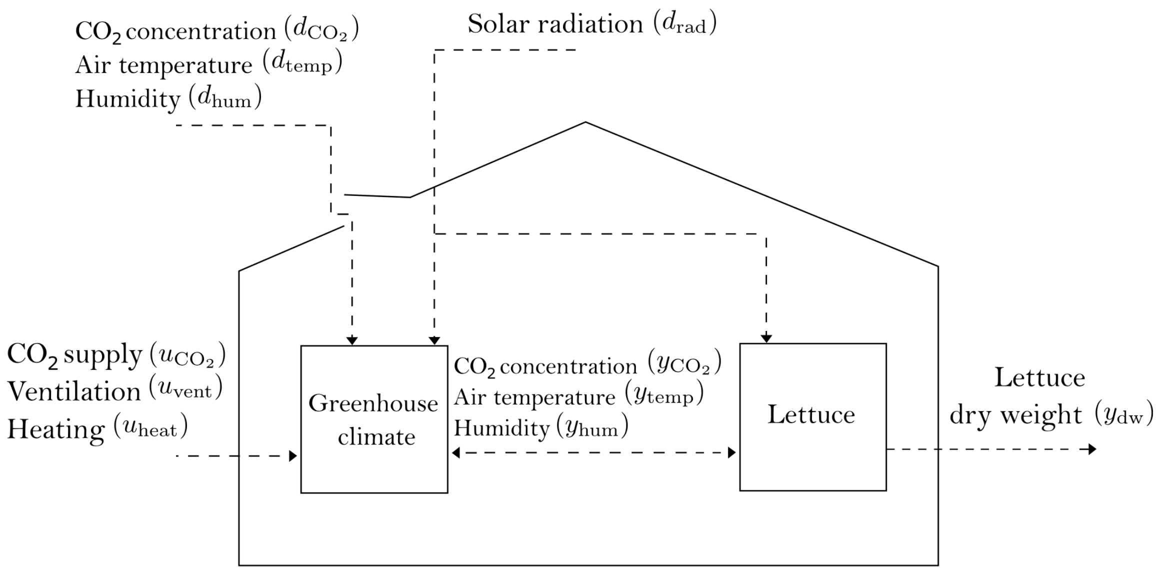

Figure 2-1: Illustration of the lettuce greenhouse model [56].

2-1-2 The Economics and the Constraints

The economical optimization of the greenhouse depends on maximizing revenue from the dry weight of the lettuce while minimizing the operational costs due to heating and carbon dioxide injection. The costs associated with ventilation are due to the electric motors changing the angle of the windows and are considered negligible. Van Henten [60] found the auction price of lettuce to be highly correlated with its weight and uses the linear relation $P_{\text{dw}} = q_{p,1} + q_{p,2}x_{\text{dw}}$ to approximate it. He derives the cost of heating by considering the cost of natural gas that provides an equivalent amount of heat when burned. The total cost of a growth period can therefore be expressed as the following:

$$J = -q_{p,1} - q_{p,2}x_{\text{dw}}(t_f) + \int_{t_0}^{t_f} q_{\text{CO}_2}u_{\text{CO}_2}(t) + q_{\text{heat}}u_{\text{heat}}(t)\, dt, \tag{2-2}$$

with

$$q_{p,1} = 180\,\text{ct}, \quad q_{p,2} = 1600\,\text{ct/kg}, \quad q_{\text{CO}_2} = 4.2 \cdot 10^{-5}\,\text{ct/mg}, \quad q_{\text{heat}} = 6.35 \cdot 10^{-7}\,\text{ct/W}.$$

Some effects that are not included in the model such as the effect of humidity on plant growth can be accounted for by placing constraints around known ideal operating regions. Controlling the humidity is a crux of the control problem, as the inputs do not permit direct influence over humidity. High humidity ($> 90\%$) and condensation can increase the risk of fungal disease [20] while low humidity ($< 50\%$) can hinder carbon dioxide uptake and therefore photosynthesis [59]. Temperatures above 40°C can be fatal for lettuce and below 5°C are avoided According to Van Henten [60] moreover, he uses a higher lower bound on the temperature to prevent numerical errors due to the model. The inclusion of carbon injection is meaningful as another point of economic optimization. Carbon dioxide comes at a cost, but quickens plant growth under light. Another such inclusion might have been a model of artificial lighting [34] but this may also distract from the importance of solar irradiation. A reasonable upper bound for carbon dioxide is a generous 1500 ppm, above which is unlikely to be optimal, as it is expensive to maintain and has a marginal effect. Further constraints are related to the physical limits of the inputs, values of which are also provided for the setup in Van Henten [60]. Reasonable constraints for greenhouse lettuce farming are listed below.

- $0\,\text{ppm} \leq y_{\text{CO}_2} \leq 1500\,\text{ppm}, \quad 0\,\text{mg/m}^2\text{s} \leq u_{\text{CO}_2} \leq 1.2\,\text{mg/m}^2\text{s}$
- $6.5°\text{C} \leq y_{\text{temp}} \leq 35°\text{C}, \quad 0\,\text{W/m}^2 \leq u_{\text{heat}} \leq 150\,\text{W/m}^2$
- $50\% \leq y_{\text{hum}} \leq 90\%, \quad 0\,\text{mm/m}^2\text{s} \leq u_{\text{vent}} \leq 7.5\,\text{mm/m}^2\text{s}$

Output constraints would not be necessary if the model represented reality adequately. Such a model would likely be hard to manipulate and simulate due to its size, even if it were possible for such a model to be constructed. In reality, plant physiology and many other important factors that affect greenhouse farming are not precisely understood. In their place, rules of thumb derived from experience and empirical evidence can be incorporated through constraints. More relaxed constraints allow for more freedom in the optimization while risking unmodelled detrimental effects. A good balance is key for safe and economical operation. The greenhouse system can tolerate small violations. That allows more freedom for controller design as opposed to a system that requires hard constraints, such that they may lead to catastrophic failure when violated.

Table 2-2: Values of Constant Model Parameters [60].

Parameter	Value	Parameter	Value	Parameter	Value	Parameter	Value
$c_{1,1}$	0.544	$c_{2,1}$	4.1	$c_{3,1}$	$3 \cdot 10^4$	$c_{4,1}$	4.1
$c_{1,2}$	$2.65 \cdot 10^{-7}$	$c_{2,2}$	$4.87 \cdot 10^{-7}$	$c_{3,2}$	1290	$c_{4,2}$	0.0036
$c_{1,3}$	53	$c_{2,3}$	$7.5 \cdot 10^{-6}$	$c_{3,3}$	6.1	$c_{4,3}$	9348
$c_{1,4}$	$3.55 \cdot 10^{-9}$	$c_{2,4}$	8.31	$c_{3,4}$	0.2	$c_{4,4}$	8314
$c_{1,5}$	$5.11 \cdot 10^{-6}$	$c_{2,5}$	273.15			$c_{4,5}$	273.15
$c_{1,6}$	$2.3 \cdot 10^{-4}$	$c_{2,6}$	101325			$c_{4,6}$	17.4
$c_{1,7}$	$6.29 \cdot 10^{-4}$	$c_{2,7}$	0.044			$c_{4,7}$	239
$c_{1,8}$	$5.2 \cdot 10^{-5}$					$c_{4,8}$	17.269
						$c_{4,9}$	238.3

2-2 Model Predictive Control

The Model Predictive Control framework has seen success in a wide range of control applications [44][50] which is due to its conceptual simplicity alongside its ability to handle constrained multivariable problems. Fundamentally, MPC relies on a model of the system to make predictions about the future states of the system, an optimization problem is solved on-line to find the inputs that lead to the most desirable predictions. The algorithm is applied in a receding horizon fashion whereby the optimization problem is solved for a certain amount of time/steps into the future, the first input is applied to the system and the whole process is repeated starting from the newly observed states such that the new prediction horizon is shifted one step. In its traditional form its formulation is similar to a linear-quadratic regulator (LQR), though with a finite horizon. Unlike the LQR where the full state feedback gain matrix can be calculated analytically by solving the algebraic Riccati equation, the inputs are calculated through a multi-step optimization problem. Therefore, constraints can be easily introduced for the states and inputs.

For a system with states $x \in \mathbb{R}^n$ and inputs $u \in \mathbb{R}^m$ whose dynamics are described by $f : \mathbb{R}^n \times \mathbb{R}^m \to \mathbb{R}^n$ such that $x^+ = f(x, u)$, the general nominal MPC formulation for a single step is given below [39]. The N-step cost function $V_N := V_f(x_N) + \sum_{i=0}^{N-1} \ell(x_i, u_i)$ consists of the stage cost $\ell : \mathbb{R}^n \times \mathbb{R}^m \to \mathbb{R}$ incurred at each step and the terminal cost associated with the value of the final state $V_f : \mathbb{R}^n \times \mathbb{R}^m \to \mathbb{R}$.

$$
\begin{aligned}
&\min_{\mathbf{u}} \; V_f(x_N) + \sum_{i=0}^{N-1} \ell(x_i, u_i) \\
&\text{subject to} \\
&\qquad x_0 = x \\
&\qquad x_{i+1} = f(x_i, u_i)\,, \quad \forall i \in \mathbb{I}_{[0:N-1]} \\
&\qquad (x_i, u_i) \in \mathbb{Z}\,, \quad \forall i \in \mathbb{I}_{[0:N-1]} \\
&\qquad x_N \in \mathbb{X}_f
\end{aligned}
$$

A control sequence $\{u(0), u(1), ..., u(N-1)\}$ is denoted by $\mathbf{u}$. The states at step i are determined by the inital state x and control sequence $\mathbf{u}$, and are denoted by x_i. The initial state and the dynamics are formulated as constraints. The set $\mathbb{Z} \subseteq \mathbb{X} \times \mathbb{U}$ imposes the remaining constraints on the states and inputs, when these constraints are independent of each other they are described by the closed set $\mathbb{X}$ and the compact set $\mathbb{U}$. The control law is given by the first input in the optimal input sequence $\mathbf{u}^0(x)$ resulting in the optimal cost $V_N^0(x) := V_N(x, \mathbf{u}^0(x))$.

$$
\kappa_N(x) := u^0(0; x)
$$

The terminal cost V_f and the terminal set $\mathbb{X}_f$, which imposes a constraint on the final state in the horizon, are employed for stability analysis. The terminal cost V_f should approximate the infinite-horizon cost in the neighbourhood of the terminal set so that $V_N^0(x) \approx V_\infty^0(x)$. Using a Lyapunov function as the terminal cost, Mayne et al. [40] showed that under reasonable assumptions the following ensures asymptotic stability.

- $\mathbb{X}_f \subseteq \mathbb{X}$, $\mathbb{X}_f$ closed, $0 \in \mathbb{X}_f$ (the terminal set contains the origin and satisfies state constraints).

- $\kappa_f(x) \in \mathbb{U}$, $\forall x \in \mathbb{X}_f$ (input constraints satisfied by the control law in the terminal set).
- $f(x, \kappa_f(x)) \in \mathbb{X}_f$, $\forall x \in \mathbb{X}_f$ (the terminal set is positively invariant under the control law).
- $\exists \mathcal{K}_\infty$ function α such that $\ell(x, \kappa_f(x)) \geq \alpha(|x|)$
- $V_f(f(x, \kappa_f(x))) \leq V_f(x) - \ell(x, \kappa_f(x))$, $\forall x \in \mathbb{X}_f$ (the terminal cost is a local Lyapunov function whose value decreases faster than the stage cost).

With all the above, the following can be shown.

$$V_N^0(f(x, \kappa_N(x))) \leq V_N^0(x) - \ell(x, \kappa_N(x))$$

The formulation given here formulation is for a regulation problem with the desired states at the origin. The optimal cost will decrease at each step until the states converge at the origin.

The traditional MPC regulator considers a linear system with linear constraints and a cost function that is quadratic in the states and inputs with respective positive semi-definite weighting matrices Q, R and P as given below.

$$\begin{aligned} \min_{\mathbf{u}} \; & \underbrace{x_N^T P x_N}_{V_f(x_N)} + \sum_{k=0}^{N-1} \underbrace{x_k^T Q x_k + u_k^T R u_k}_{\ell(x_i, u_i)} \\ \text{subject to} \; & \\ x_0 &= x \\ x_{k+1} &= A x_k + B u_k \,, \quad \forall k \in \mathbb{I}_{[0:N-1]} \\ C x_k + D u_k &\leq h_x \,, \quad \forall k \in \mathbb{I}_{[0:N-1]} \\ Y x_N &\leq h_f \end{aligned} \tag{2-3}$$

The LQR infinite-horizon cost is a natural choice for the terminal cost and makes the controller trivially equivalent to an LQR when there are no constraints. The problem can be reformulated such that it be quickly and efficiently solved by quadratic programming. Defining the following where $\otimes$ denotes the Kroenecker product:

$$\begin{gathered} \mathbf{A} := \begin{bmatrix} A^0 \\ A^1 \\ A^2 \\ \vdots \\ A^N \end{bmatrix}, \mathbf{T} := \begin{bmatrix} 0 & 0 & \cdots & 0 \\ I & 0 & \cdots & 0 \\ A & I & \ddots & \vdots \\ \vdots & \vdots & \ddots & 0 \\ A^{N-1} & A^{N-2} & \cdots & I \end{bmatrix}, \mathbf{B} := \mathbf{T} \otimes B, \; \mathbf{C} := \begin{bmatrix} I_N \otimes C & 0 \\ 0 & Y \end{bmatrix}, \\ \mathbf{D} := \begin{bmatrix} I_N \otimes D \\ 0 \end{bmatrix}, \; \mathbf{Q} := \begin{bmatrix} I_N \otimes Q & 0 \\ 0 & P \end{bmatrix}, \; \mathbf{R} := I_N \otimes R \end{gathered} \tag{2-4}$$

the state sequence is given by the following.

$$\mathbf{x}_{0:N} = \mathbf{A} x + \mathbf{B} \mathbf{u}_{0:N-1}$$

The optimization problem in 2-3 can then be reformulated defining the following where $\mathbf{1}_N$ denotes a column vector of ones of length N,

$$H = \mathbf{B}^T\mathbf{Q}\mathbf{B} + \mathbf{R}, \quad c^T = x_0^T\mathbf{A}^T\mathbf{Q}\mathbf{B}$$
$$G = \mathbf{C}\mathbf{B} + \mathbf{D}, \quad h_{\mathbf{u}} = \begin{bmatrix} \mathbf{1}_N \otimes h_x \\ h_f \end{bmatrix} - \mathbf{C}\mathbf{A}x$$

resulting in the quadratic programming problem given below. Notably, the states are no longer an optimization variable as they are fully determined by the initial states, the dynamics and the inputs. In this form the dynamics are accounted for by the cost function instead of the constraints.

$$\begin{aligned} \min_{\mathbf{u}} \ & \frac{1}{2}\mathbf{u}^T H\mathbf{u} + c^T\mathbf{u} \\ \text{subject to} & \\ & G\mathbf{u} \leq h_{\mathbf{u}} \end{aligned} \tag{2-5}$$

Quick calculations are often necessary for on-line application on sampled-data systems with fast dynamics where the calculation has to be made between each sample. The dynamics of non-linear systems are commonly linearized for easier calculation. Ghoumari et al. [21] use such a method for greenhouse climate control and demonstrate better performance compared to an adaptive PID controller. The errors introduced in the linearization is mitigated by the feedback. In some cases however, this proves insufficient and the use of a non-linear model in the optimization is necessary. The economical optimization of the greenhouse climate control is one such problem due to the non-linearities in the dynamics. Another source of difficulty is the difference in time scale between the greenhouse climate and plant growth dynamics.

2-2-1 Economic Model Predictive Control

The economic optimization is usually done off-line in real-time optimization where desired set points are calculated to be fed into a tracking controller. A tracking MPC with a tunable quadratic cost will treat any deviation from the predetermined trajectory as unfavorable, even if the deviation is more profitable. Incorporating the economics into the optimization problem of the controller can improve economic performance by managing fast transient dynamics better and removing the errors due to any differences between the model used in the optimization and in the control. This is achieved by using a cost that reflects the economic cost and is referred to as economic MPC [22]. For the case of the greenhouse climate optimization a natural choice for the cost is a linear weighting of all the inputs according to their costs and a negative weighting of the increase in lettuce dry weight as in Equation 2-2.

$$V_N(x_0, \mathbf{u}) = \sum_{i=0}^{N-1} \underbrace{q_{p,2}(x_{\mathrm{dw},i} - x_{\mathrm{dw},i+1}) + \begin{bmatrix} q_{CO_2} & q_{vent} & q_{heat} \end{bmatrix} u_i}_{\ell(x_i, u_i)}$$

EMPC requires an altered stability analysis as the loss is no longer a measure of the distance between the current state and the desired state. Amrit et al.[1] use an assumption of strict dissipativity to show stability. This requires the existence of a storage function $\lambda : \mathbb{X} \rightarrow \mathbb{R}$

and a function $\rho : \mathbb{X} \to \mathbb{R}_{\geq 0}$ which is zero at the origin and positive otherwise (i.e. positive definite) such that the following is true under the EMPC:

$$\lambda(f(x, \kappa_N(x))) - \lambda(x) \leq -\rho(x - x_s) + \ell(x, u) - \ell(x_s, u_s),$$

where x_s and u_s are the optimal steady state values. The existence of such functions cannot be easily shown for a greenhouse climate system due to the unstable growth dynamics and is likely not possible. Moreover, steady state is not desirable in this setting as that would correspond to stopping the growth of the plant. Any stability analysis will be further complicated when uncertainties and the effect of exogenous inputs are taken into consideration.

2-3 Stochastic and Robust MPC

The greenhouse optimization problem will benefit from considering uncertainties as it essentially relies on uncertain weather predictions [33]. So far the discussion has been contained to nominal MPC where the dynamics are deterministic. Such a controller is bound to lead to errors due to disturbances, simplifications in the model, and statistical errors in the system identification process. When these errors are small nominal MPC is sufficient to control the system with adequate feedback. However, uncertainties will inevitably lead to constraint violations. In some applications this can be tolerated, in some others violations can be mitigated by setting more conservative constraints. In applications where safety is of utmost importance, robust MPC is a way to vastly improve constraint compliance by taking the uncertainties into account.

2-3-1 Robust Model Predictive Control

Robust MPC includes disturbances in the model ($x^+ = f(x, u, w)$), defines a set of possible disturbances $w \in \mathbb{W}$ and assures constraint compliance under all possible disturbance realizations within that set [5]. The cost function can remain the same with zero disturbance, or it can be replaced by the maximum cost [13].

$$V_N(x_0, \mathbf{u}) := \max_{\mathbf{w} \in \mathbb{W}^{N-1}} V_f(x(N; x_0, \mathbf{u}, \mathbf{w})) + \sum_{i=0}^{N-1} \ell(x(i; x_0, \mathbf{u}, \mathbf{w}), u(i))$$

Both methods use the following robust constraint on the states.

$$x(i; x_0, \mathbf{u}, \mathbf{w}) \in \mathbb{X}, \quad \forall i \in \mathbb{I}_{[0:N]}, \quad \forall \mathbf{w} \in \mathbb{W}$$

Minimizing over control policies would be preferable in an uncertain setting as the structure of the policy can aid robustness and tractability as opposed to a free control sequence. A policy can also enable the control law to incorporate information about past and current states and disturbances. One way to achieve this is to supplement the input with a linear feedback law. Rossiter et al.[52] proposed calculating a stabilizing gain beforehand and adding it to the input ($u = -Kx + v$). This is not very useful for economic MPC where stability is harder to define. A feedback law can also be calculated on-line in the following affine parametrization where g and L are the decision variables.

$$u(i) = g(i) + \sum_{j=0}^{i} L(i, j)x(j)$$

Imposing this constraint often leads to nonconvexities in the constraints. For linear systems with additive disturbances, Goulart et al.[24] show that a disturbance feedback parametrization avoids this problem and that there is a one-to-one nonlinear mapping between the two parametrizations. In distrubance feedback parametrization, the past disturbances affect the input linearly as shown below.

$$u(i) = v(i) + \sum_{j=0}^{i-1} M(i, j)w(j)$$

Considering additive disturbance on the states by replacing the equality constraints in 2-3 with

$$x_{k+1} = Ax_k + Bu_k + w_k$$

and disturbance feedback with the equality constraint,

$$\mathbf{M} := \begin{bmatrix} 0 & \cdots & \cdots & 0 \\ M_{1,0} & 0 & \cdots & 0 \\ \vdots & \ddots & \ddots & \vdots \\ M_{N-1,0} & \cdots & M_{N-1,N-2} & 0 \end{bmatrix}$$
$$\mathbf{u} = \mathbf{M}\mathbf{w} + \mathbf{v}$$

the constraints can be rewritten using definitions from 2-4 and defining the following:

$$F := \mathbf{CB} + \mathbf{D}, \quad G := \mathbf{CT}, \quad H := -\mathbf{CA}, \quad c := \begin{bmatrix} \mathbf{1}_N \otimes h_x \\ h_f \end{bmatrix}$$

Which results in the following convex and linear constraint.

$$F\mathbf{v} + (F\mathbf{M} + G)\mathbf{w} \leq c + Hx \tag{2-6}$$

Using the state feedback formulation

$$\mathbf{L} := \begin{bmatrix} L_{0,0} & 0 & \cdots & 0 \\ \vdots & \ddots & \ddots & \vdots \\ L_{N-1,0} & \cdots & L_{N-1,N-1} & 0 \end{bmatrix}$$
$$\mathbf{u} = \mathbf{L}\mathbf{x} + \mathbf{g},$$

the state sequence and therefore the control sequence can be written as the following which always has an equivalent distrubance feedback paramterization since‘ **BL** strictly lower-triangular.

$$\mathbf{x} = (I - \mathbf{BL})^{-1}(\mathbf{Bg} + \mathbf{Tw} + \mathbf{A}x_0)$$
$$\mathbf{u} = \underbrace{L(I - \mathbf{BL})^{-1}\mathbf{T}}_{\mathbf{M}}\,\mathbf{w} + \underbrace{L(I - \mathbf{BL})^{-1}(\mathbf{Bg} + \mathbf{A}x_0) + g}_{\mathbf{v}}$$

Robust MPC results in a conservative control law, especially in the maximum cost setting where the controller is optimized to operate under the worst case disturbance realization which is often improbable. Using a nominal cost is a better choice in many applications as it optimizes the controller to operate in an average disturbance realization while still ensuring constraint compliance in the worst case. However, both methods may lead to infeasible problems when the constrained inputs are not sufficient to deal with a highly unlikely extreme disturbance. Although desirable for safety, a conservative law is detrimental to optimality. This is addressed by stochastic MPC explained in the following Section.

2-3-2 Stochastic Model Predictive Control

Stochastic MPC assumes the disturbances follow a certain probability distribution in addition to belonging in a certain set. Hard constraints are replaced by chance constraints that allow a certain probability of violation $\epsilon \in [0,1]$ [54]. A linear SMPC problem then, may look like the following with the disturbance feedback parametrization [23].

$$\begin{aligned} \min_{\mathbf{M},\mathbf{v}} \ & \mathbb{E}_{\mathbb{P}_w}\left[V_f(x_N) + \sum_{i=0}^{N-1} \ell(x_i,u_i)\right] \\ \text{subject to} \ & \\ \mathbf{u} &= \mathbf{M}\mathbf{w} + \mathbf{v} \\ x_0 &= x \\ x_{i+1} &= Ax_i + B_u u_i + B_w w_i\,, \quad \forall i \in \mathbb{I}_{[0:N-1]} \\ (x_{i+1}, u_i) &\in \mathbb{X} \times \mathbb{U}, \quad \forall i \in \mathbb{I}_{[0:N-1]} \\ w_i &\sim \mathbb{P}_w \\ \mathbb{P}_w(x_i \in \mathbb{X}) &\geq 1 - \epsilon, \quad \forall i \in \mathbb{I}_{[1:N]} \end{aligned} \tag{2-7}$$

Here the disturbances are assumed to be additive which is the most commonly encountered and studied case. Multiplicative disturbances are also considered [7][49].

Analytic Reformulation of Chance Constraints

Linear independent chance constraints are sufficient to place bounds on the states and at the same time allow easy calculation. The state can be represented as the sum of a nominal state which disregards any disturbances and an error term $x = \bar{x} + e$. Due to the linear dynamics the error is a linear function of the disturbance sequence $e_i = E_i\mathbf{w}$. The value of E_i can be calculated based on the choice of input parametrization, For disturbance feedback it is given by the columns of $\mathbf{E}$ in the following equation using a similar notation to 2-4.

$$\mathbf{e} = \underbrace{(\mathbf{B}_u\mathbf{M} + \mathbf{B}_w)}_{\mathbf{E}}\,\mathbf{w}$$

The chance constraint can now be written as the following.

$$\mathbb{P}(g^T(\bar{x}_i + E_i\mathbf{w}) \leq h) \geq 1 - \epsilon, \quad \forall i \in \mathbb{I}_{[0:N]}$$

This constraint can be replaced by a hard constraint using the probability density of the disturbance to find the value of the probable deviation q.

$$q_i(1-\epsilon) := \operatorname*{argmin}_q q, \quad \text{s.t. } \mathbb{P}(g^T E_i\mathbf{w} \leq q) \geq 1 - \epsilon \tag{2-8}$$

A hard constraint accounting for the probable deviation can be used to replace the chance constraint.

$$g^T\bar{x}_i \leq h - q_i(1-\epsilon), \quad \forall i \in \mathbb{I}_{[0:N]} \tag{2-9}$$

If the error is Gaussian with zero mean and covariance matrix Σ, a simple expression is available using the cumulative density function for the normal distribution Φ and $\mathbf{\Sigma} = \text{diag}(\Sigma, ..., \Sigma)$ [47].

$$q_i(1-\epsilon) = \sqrt{g^T E_i \mathbf{\Sigma} E_i^T g}\, \Phi^{-1}(1-\epsilon)$$

If however, the mean and covariance is known but the distribution is unknown or not Gaussian, Chebyshev's inequality [38] can provide an upper bound such as the following when the mean is zero.

$$q_i(1-\epsilon) \leq \sqrt{g^T E_i \mathbf{\Sigma} E_i^T g} \sqrt{\frac{1-\epsilon}{\epsilon}}$$

Cannon, Kouvaritakis et al.[14][32] propose a tube-based method rooted in RMPC [16][41] for linear systems with bounded disturbances where they represent the uncertainty as ellipsoidal sets around a nominal trajectory. This follows from the separation of the state into a nominal state and the error. They also show recursive feasibility throughout the prediction horizon under tighter constraints using a pre-stabilizing feedback gain and assuming a bounded disturbance. This is achieved by modifying the definition of the probable deviation q in Equation 2-8, which only ensures feasibility at the current time, by adding the potential effect of the worst case disturbance realization during the prediction horizon.

$$\tilde{q}_i(p) := q_i(p) + \max_{\mathbf{w} \in \mathbb{W}} \sum_{j=1}^{i-1} g^T E_j \mathbf{w}$$

Their method results in a scheme with low computational load through the offline computation of the stochastic tubes. Lorenzen et al.[35] introduce a constraint only on the first step to ensure recursive feasibility without excessively shrinking the feasible region. This is done by adding a constraint such that the states must land in a robust control invariant set within the constraint set after the first step. A robust control invariant set is a set where the next states can be ensured to remain within the set under all possible disturbances while the inputs remain within their constraints. Such a set can be calculated by defining

$$C_{N,x}^{i+1} = \left\{ x \in C_{N,x}^{i} \;\middle|\; \begin{array}{l} \exists u \text{ s.t. } (x,u) \in C_N^0 \\ Ax + Bu \in C_{N,x}^{i} \ominus B_w \mathbb{W} \end{array} \right\}$$

where C_N^0 denotes the N-step constraint set and $\ominus$ stands for the Pontryagin set difference defined as: $A \ominus B := \{a \,|\, a + b \in A,\, b \in B\}$. The basis of calculating a robust invariant set $C_{N,x}^{\infty}$ is recursively calculating $C_{N,x}^{i+1}$ until $C_{N,x}^{i+1} = C_{N,x}^{i}$.

Hewing et al.[27] use a method of indirect feedback whereby they use a feedback law which is linear in the error.

$$u(i) = Ke(i) + v(i)$$

Moreover, the nominal state is not updated to the measured state and is kept separate, the initial error is often non-zero as opposed to all the other schemes. Consequently, the measured state has no direct influence on the input, only indirectly through the cost function. This enables a notion of recursive feasibility with the use of a nominal invariant set, even under unbounded disturbances.

Joint Chance Constraints

The viable set $\mathbb{X}_p$ used in Equation 2-7 for the chance constraints can be represented with a function as an inequality constraint for practicality.

$$\mathbb{P}(g(x_i) \leq 0) \geq 1 - \epsilon, \quad \forall i \in \mathbb{I}_{[0:N]}$$

When $g(\cdot)$ is simply a scalar it posits an independent constraint. If it is a vector it represents a joint chance constraint which often leads to intractable problems. They can instead be more conservatively represented by multiple independent constraints whose constraint violation probabilities add up to ϵ. For linear dependent constraints this is shown below where g_r, h_r and x_r denote the rows of G, h and x.

$$\mathbb{P}(Gx \leq h) \geq 1 - \epsilon \iff \mathbb{P}(Gx > h) < \epsilon$$

Starting from the trivial expression above and applying Boole's inequality to replace the original constraint with its rows as independent constraints results in the following.

$$\mathbb{P}(Gx > h) \leq \sum_{r=1}^{n} \mathbb{P}(g_r^T x_r > h_r) < \epsilon \Longleftarrow \mathbb{P}(g_r^T x_r > h_r) < \epsilon_r \ \forall r, \ \sum_{r=1}^{n} \epsilon_r = \epsilon$$

$$\therefore \mathbb{P}(g_r^T x_r \geq h_r) < 1 - \epsilon_r \ \forall r, \ \sum_{r=1}^{n} \epsilon_r = \epsilon \Longrightarrow \mathbb{P}(Gx \leq h) \geq 1 - \epsilon$$

The individual violation probabilities can be free variables for the optimization or they can be set equal to each other ($\epsilon_r = \epsilon/n$) which results in a more conservative reformulation.

Conditional Value-at-Risk Constraints

Following the work of Zymler et al.[68] which consider distributionally robust optimization problems with individual and joint chance constraints, Van Parys et al. [63] show that chance constraints can be formulated as conditional value at risk (CVaR) [51] constraints which result in tractable problems for linear systems. Value at risk (VaR) is defined with a loss function L^α such that $L^\alpha(x) \leq 0, \ \forall x \in \mathbb{X}_p$, quadratic losses are used in the paper.

$$\mathbb{P}\text{-VaR}_\epsilon(L^\alpha(x)) := \inf\{\gamma \in \mathbb{R} \mid \mathbb{P}(L^\alpha(x) > \gamma) \leq \epsilon\}$$

VaR corresponds to the loss that is expected to not be exceeded with probability $1 - \epsilon$ and can be used to reformulate a chance constraint.

$$\mathbb{P}\text{-VaR}_\epsilon(L^\alpha(x)) \leq 0 \iff \mathbb{P}(x \in \mathbb{X}_p) \geq 1 - \epsilon$$

However, VaR is not convex in L^α which can be remedied by using CVaR instead.

$$\mathbb{P}\text{-CVaR}_\epsilon(L^\alpha(x)) := \inf_{\beta \in \mathbb{R}} \{\beta + \frac{1}{\epsilon} \mathbb{E}_\mathbb{P} \left[L^\alpha(x) - \beta\right]\}$$

CVaR corresponds to the expected loss in the worst cases with probability ϵ as shown in Figure 2-2, it provides an upper bound to VaR and is more conservative as a result. An advantage of these formulations is that they penalize not only the violations but also the amount of which the constraint is violated through the loss function. As such, not only is the frequency of violations restricted but also the extent.

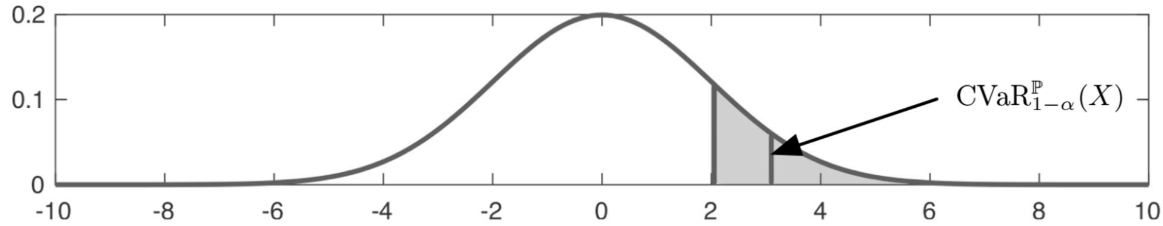

Figure 2-2: Depiction of the conditional value at risk at level $\alpha = 0.15$ for a Gaussian random variable X. The first line corresponds to the value at risk as the shaded region accounts for $\alpha \times 100\%$ of the mass of the Gaussian distribution [18].

Average Constraint Violation Constraints

Oldewurtel et al.[46] propose using adaptive constraints to make the empirical violation probabilities converge to the desired probabilities and establish convergence guarantees for certain linear systems. They relax the constraints when there are less violations than expected, and vice versa. Korda et al.[31] use the same strategy to constrain the expected average constraint violation. The average constraint violation is formulated using the weighted average amount of violation accumulated v_t/s_t with the following.

$$v_t := \sum_{k=0}^{t} \gamma^{t-k} l(g^T x_{t+1} - h), \quad t \in \mathbb{I}_{\geq 0}$$

$$s_t := \sum_{k=0}^{t} \gamma^{t-k}, \quad t \in \mathbb{I}_{\geq 0}$$

If the loss function $l(\cdot)$ is chosen as the indicator function of the positive real line, the resulting constraint will correspond to limiting the probability of violation. However, unlike the previously mentioned stochastic constraints which are imposed pointwise in time, average violation constraints are imposed on the closed loop process as a whole. Alternatively, the loss function can be chosen as $l(\cdot) = \max\{\cdot, 0\}$ to penalize violations in proportion to the amount of violation, more similar to a CVaR constraint. Starting from a small amount of allowed violation $\alpha < \xi$, which results in a constraint that can be represented as

$$\mathbb{E}_t[l(g^T x_{t+1} - h)] \leq \alpha,$$

they introduce an additional constraint on the average violation

$$\mathbb{E}_t\left[\frac{v_{t+1}}{s_{t+1}}\right] \leq \xi.$$

Together these result in the constraint

$$\mathbb{E}_t[l(g^T x_{t+1} - h)] \leq \beta_t,$$

where

$$\beta_t := \max(\gamma(\xi s_t - v_t) + \xi, \alpha).$$

The constraint is relaxed when the average constraint violation is below the desired amount ξ and tightened to α when it exceeds it. The online adaptation of the constraint to the observed violation results in a reduction in conservatism.

Scenario-Based Reformulation of Chance Constraints

Another way to deal with chance constraints is through the use of Monte Carlo methods where constraints are placed on a number (N_s) of possible realizations of the probabilistic variable $\mathbf{w}$ generated from the expected probability distribution [6][11].

$$g^T(\bar{x}_i + E_i\mathbf{w}_s) \leq h, \quad \forall i \in \mathbb{I}_{[0:N]}, \quad \forall s \in \mathbb{I}_{[0:N_s]}$$

An advantage of this method is its natural ability to deal all types of probability distributions and joint chance constraints.

Given the number of scenarios, statistical upper bounds can be obtained on the probability that the chance constraint does not hold (β) as in 2-10, where d is the dimension of optimization variable in the scenario-based MPC problem. Defining the violation probability $V(x_s^*)$ as the probability of constraint violation when the inputs are optimized for a certain sampled set of scenarios and then applied under a disturbance with the same distribution, an upper bound is given by the following expression [12].

$$\mathbb{P}(V(x_s^*) > \epsilon) < \beta \leq \sum_{j=0}^{d-1} \binom{N_s}{j} \epsilon^j (1-\epsilon)^{N_s - j} \tag{2-10}$$

This can be used to select an appropriate value for the number of scenarios (N_s), as high values can be prohibitive due to the required computing power. Using too many samples can also lead to excessively conservative controllers. Scildbach et al.[53] remove unlikely outliers with extreme disturbances from the scenarios considered for less conservative control laws at the cost of needing more realizations for the same guarantees.

Nonlinear Systems

Scenario-based methods are often preferred for nonlinear models [25] as tracking the propagation of stochastic uncertainty through the system dynamics is challenging. Weissel et al.[66] use Gaussian mixtures to represent the uncertainty, Mesbah et al.[43] propose a nonlinear SMPC using polynomial chaos expansions. The scheme works by using samples to calculate the appropriate coefficients for a polynomial chaos expansion made up polynomial basis functions for the relation between the uncertain variables and the resulting states. The polynomials are chosen to be orthogonal to each other with respect to the probability distribution of the uncertainty. The orthogonality of the basis functions allow for easy calculations of the statistical moments of the system which are then used in the constraints. Van Hessem and Bosgra [62] introduce a method where they optimize a nonlinear deterministic trajectory and use that trajectory to obtain linearization points and references for linear SMPC. This results in a linear time-varying system in the SMPC prediction horizon and mitigates the errors introduced in linearization. When there are no disturbances, this scheme is expected to follow the nonlinear feedforward trajectory as both problems use the same cost. When there are disturbances, the linear SMPC will try to counteract their effect. It is also possible to use the same cost in the SMPC as in the calculation of the optimal trajectory, so that it may exploit disturbances to reduce cost.

Some Applications

Oldewurtel et al.[45] apply SMPC with the disturbance feedback parametrization on a linearized model for building climate control. Their work also depends on weather predictions and they demonstrate better performance with SMPC over nominal MPC and over a rule based controller especially in constraint compliance. They represent the error in the weather forecast using an autoregressive model with Gaussian noise $w_i \sim \mathcal{N}(0, I)$.

$$e_{i+1} = Fe_i + Kw_i$$

Their cost also reflects the economics though it is simpler compared to the greenhouse problem as the only cost is the cost of the inputs whereas the growth of the plant plays an important role for the greenhouse economics. Ma et al.[36] report promising experimental results for SMPC in building climate control. Zhang et al.[67] tackle a similar problem using a scenario-based approach.

Parisio et al.[48] use a higher level nominal MPC based on forecasts for optimization on a mixed logical dynamical model and a lower level SMPC to deal with disturbances in the control of a microgrid with multiple power sources following the optimal trajectory. They demonstrate performance improvements over deterministic schemes in experiments. Cominesi et al.[17] tackle a similar problem but use different timescales for the two controllers. They also implement a scenario-based lower level controller with marginally worse results. They work with accurate predictions, the error is close to zero mean. The separate control structure can lead to economic losses when more significant uncertainties are present. They propose updating the higher-level planning more often to better deal with such situations.

Chen and You [15] propose a robust MPC approach for greenhouse farming under harsh climate conditions. The work adopts data-driven approaches to create uncertainty sets that allow a small probability of constraint violation. They apply principal component analysis on historical weather prediction error data and create uncertainty sets using Gaussian kernels. They show better control cost compared to standard robust MPC while assuring adequate constraint compliance.

Kuijpers et al. [33] investigate the weather forecast error and use a combination of a Kalman filter to estimate error and a scenario-based robust MPC to control a greenhouse climate system. They find that the Kalman filter reduces the amount of constraint vioations without any significant effect on the cost. Boersma et al.[9] use the same nonlinear greenhouse model considered here, they investigate the effect of parameter uncertainty with a scenario-based nonlinear SMPC approach and conclude that the controller performance is sensitive to uncertainty which suggests that SMPC may be worthwhile. On the other hand, they find that the stochastic controller is significantly detrimental to the efficiency of the greenhouse compared with a nominal controller. Svensen et al.[56] use a linear SMPC by linearizing around the current states to control the system with uncertainty in simulation. This scheme performs adequately in a couple of studied cases in terms of reducing constraint violations. They consider the uncertainty in model parameters as following a truncated normal distribution while formulating constraints and demonstrate better constraint compliance for compared to nominal MPC especially for the humidity. They do not comment on the effect on the cost. Using a truncated distribution is effective in reducing conservativism. However, it is not clear wether this is an adequate representation for parameter uncertainty. Performance in the more challenging uncertainty realizations is likely to be wanting. Mallick et al. [37] propose a reinforcement learning-informed MPC where the MPC provides a policy structure for the RL algorithm which optimizes the parameters of the model in closed loop. Their method results in significantly better compliance with constraints at a cheaper cost compared to scenario-based methods after a hundred training cycles.

Chapter 3

Problem Statement

This thesis is concerned with the economically optimal control of the climate inside a lettuce greenhouse. More specifically, the aim is to improve constraint compliance in the presence of weather uncertainty or parametric uncertainty. The greenhouse is assumed to be described by the model due to Van Henten [60] in Equation 2-1 and discretized such that $x_{k+1} = f_d(x_k, u_k, d_k, p)$ where p is the vector of model parameters. The fourth-order Runge-Kutta method is employed in the discretization. Full state knowledge is assumed. The model is discussed in detail in Section 2-1. The input constraints and the cost are as described in Section 2-1-2. The output constraints are chosen to be closer to the previous studies as follows.

- $0\,\text{ppm} \leq y_{\text{CO}_2} \leq 1600\,\text{ppm}$
- $10°\text{C} \leq y_{\text{temp}} \leq 25°\text{C}$
- $40\% \leq y_{\text{hum}} \leq 70\%$

There are some small differences, one study [56] sets the lower bound of the humidity to zero, the lower bound on temperature to 6.5°C and has a higher upper bound on the carbon dioxide concentration. Some others [9][37] have separate temperature constraints according to the time of day (between 15-20°C during the day and 10-15°C at night). This method was not employed, as the reasoning behind separate constraints is not clear. They result in tighter constraints which are not connected to any safety concern.

$$\begin{aligned}
&\min_{\mathbf{u}} \sum_{k=0}^{N-1} - q_{p,2}(x_{\text{dw},k+1} - x_{\text{dw},k}) + \begin{bmatrix} q_{CO_2} & q_{vent} & q_{heat} \end{bmatrix} u_k \\
&\text{subject to} \\
&\qquad x_0 = x \\
&\qquad x_{k+1} = f_d(x_k, u_k, d_k, p)\,, \quad \forall k \in \mathbb{I}_{[0:N-1]} \\
&y_{\min} \leq g(x_k, p) \leq y_{\max}\,, \quad \forall k \in \mathbb{I}_{[0:N]} \\
&\quad u_{\min} \leq u_k \leq u_{\max}\,, \quad \forall k \in \mathbb{I}_{[0:N-1]}
\end{aligned} \tag{3-1}$$

When there is no uncertainty in the system a nonlinear model predictive control (NMPC) scheme as given in Equation 3-2 can adequately control the greenhouse climate. The optimization problem is solved every time step in a receding-horizon fashion and the first inputs in the solution are applied to the system. The states of a lettuce greenhouse when controlled by an NMPC in simulation are shown in Figure 3-1. The system operates on the constraint boundaries as expected from an optimal trajectory. When there is sunlight, carbon dioxide is introduced and the temperature is increased to promote plant growth. At night the greenhouse is kept at the lower temperature boundary to save on heating costs and to slow down the loss of plant mass through respiration. The humidity stays at the upper bound at most times, which indicates it is the main restriction. Reducing humidity requires increasing the temperature and/or increasing ventilation. Both of which will lead to an increase in heating requirements and therefore costs.

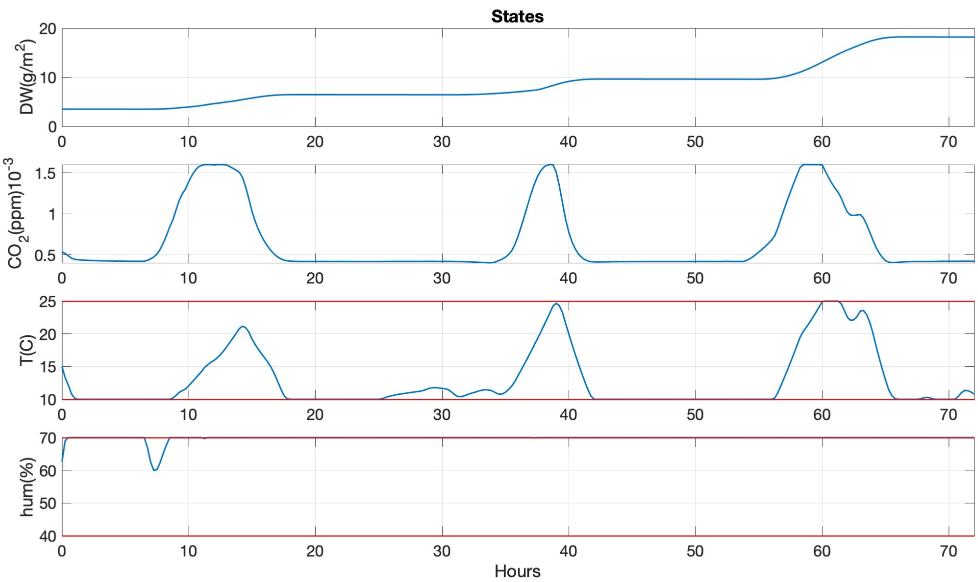

Figure 3-1: 3-Day simulation of the lettuce greenouse controlled by NMPC.

The NMPC formulation can benefit from a couple of modifications. Constraining the change in input is common and present in the previously mentioned studies. The constraint limits how aggressively the inputs can change, this results in smoother inputs which do not take as much of a toll on hardware. It also prevents erratic behaviour in some of the linearized controllers in the following chapter. The second modification is the addition of slack variables. They ensure that the optimization problem has a feasible solution even when the output constraints are not satisfied. The cost of the slack variables were chosen to be high enough to not result in any unnecessary violations in the prediction horizon. The weighting matrix λ is diagonal with the following values repeating: $\begin{bmatrix}10^{10} & 10^4 & 3 & 1\end{bmatrix} \times 10^3$. The same slack is used for all following formulations.

$$\begin{aligned}
\min_{\mathbf{u},\mathbf{s}} \ \mathbf{s}^T \boldsymbol{\lambda} \mathbf{s} + \sum_{k=0}^{N-1} - q_{p,2}(x_{\text{dw},k+1} - x_{\text{dw},k}) + \begin{bmatrix} q_{CO_2} & q_{vent} & q_{heat} \end{bmatrix} u_k \\
\text{subject to} \\
x_0 &= x \\
x_{k+1} &= f_d(x_k, u_k, d_k, p)\,, \quad \forall k \in \mathbb{I}_{[0:N-1]} \\
y_{\min} - s_k \leq g(x_k, p) &\leq y_{\max} + s_k\,, \quad \forall k \in \mathbb{I}_{[0:N]} \\
u_{\min} &\leq u_k \leq u_{\max}\,, \quad \forall k \in \mathbb{I}_{[0:N-1]} \\
-\frac{u_{\max}}{10} &\leq u_k - u_{k-1} \leq \frac{u_{\max}}{10}\,, \quad \forall k \in \mathbb{I}_{[0:N-1]} \\
s_k &\geq 0\,, \quad \forall k \in \mathbb{I}_{[0:N]}
\end{aligned} \tag{3-2}$$

The optimal trajectory is often on constraint boundaries. In the presence of uncertainty this will inevitably lead to constraint violations. The aim of this thesis is to formulate model predictive control such that it avoids excessive constraint violations in the presence of uncertainty while incurring as little additional costs as possible. More specifically, the effect of additive weather forecast uncertainty and parameter uncertainty will be considered, and the goal for the resulting controller is to ensure operation within the constraints at least 95% of the time.

3-1 Weather Forecast Uncertainty

The first source of uncertainty that comes to mind when thinking about greenhouse climate control is weather forecasts. Though more sheltered compared to open air farming, greenhouse climates are highly dependent on weather conditions. Weather forecast error $e_k = d_k - \hat{d}_k$ is often modeled as the following AR(1) model with the diagonal matrix Ψ [45][33] which was used to construct error realizations.

$$e_{k+1} = \Psi e_k + w, \quad w \sim \mathcal{N}(\mu, \Sigma)$$

The random term is assumed to have a Gaussian distribution with zero mean. The variance of the temperature forecast error was set to roughly match observations ($3\sigma \approx 4°C$). The forecast error is known to slowly drift away from zero. This informs the choice for Ψ along with the intuition that the current is closely associated with the most recent measurement. Ψ was chosen to be slightly lower than identity, so the variance does not diverge. The exact value of Ψ and Σ was chosen such that they result in a reasonable drift-to-noise ratio for the forecast error. The variance in humidity was set to roughly match the temperature in terms of its proportion to its average value in operation in the units of the model. The errors for different states were assumed to be uncorrelated because there was no data available to infer the correlation. This resulted in the following values: $\Psi = 0.98I$, $\sigma^2_{\text{temp}} = 0.04$, $\sigma^2_{\text{hum}} = 10^{-8}$. A realization of this disturbance model is shown in Figure 3-2 and the resulting constraint violations can be seen in Figure 3-3 for the same nominal weather as used in Figure 3-1.

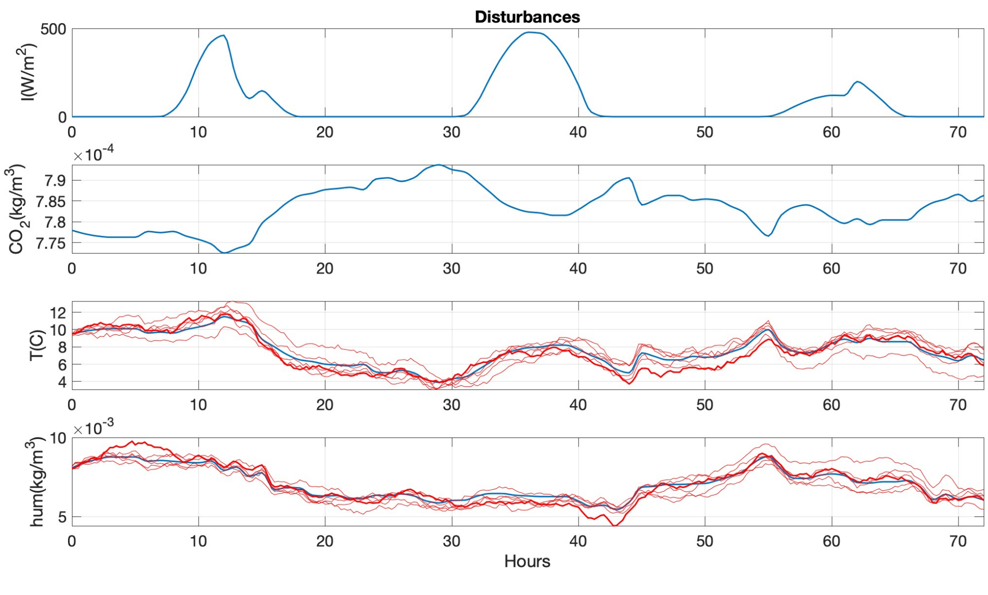

Figure 3-2: 3-Day weather forecast and some generated forecast error realizations.

The carbon dioxide concentration in the atmosphere is quite stable and it has a minor effect on the constraints, therefore it was neglected in the error modelling. The irradiation forecast error was similarly neglected as it also has a less significant effect on the constraints. Another factor in this decision was the limited information on the error of irradiation forecasts, which

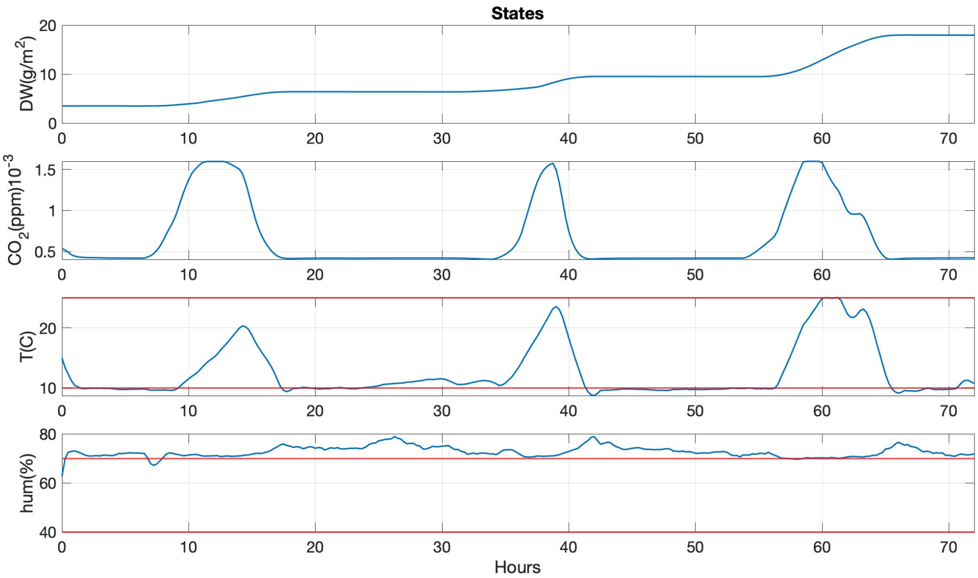

Figure 3-3: Simulation of the lettuce greenhouse controlled by NMPC with weather forecast error.

make it hard to approximate the error which is expected to be distinct enough from the other states to warrant its own error model. It deviates from the other states as the error at night is effectively zero and the irradiation error is expected to depend mostly on obstruction since the solar radiation is quite predictable.

It is important to note that weather forecasts can be very accurate and can be updated often. Moreover, in between forecast updates, the structure of the forecast error can be exploited to obtain better approximations for the weather trajectory from current measurements. Doing this in the constructed error model, for example, can reduce the error variance by a few orders of magnitude. Better weather estimations can produce significant improvements in performance by allowing less conservative controllers. It may therefore be worthwhile to target other significant sources of uncertainty with the methods of this thesis.

3-2 Parameter Uncertainty

The greenhouse model relies on 28 parameters in total, ranging from physical constants to parameters peculiar to a specific greenhouse, to parameters that can quickly change with the wind. The parameters that cannot be measured directly and the ones that are more volatile are a significant source of uncertainty in the system. Unlike weather forecasts, which are bound to err in both directions throughout the growing season, errors in the parameters may persist, resulting in a constant bias in the controller. When there are constraint violations, this bias may lead to a control input that is insufficient to bring the states back within the constraints, which will cause sustained violations as shown in Figure 3-4. The parameter error is modelled as following a uniform distribution with a maximum error of 20%.

$$p_i - \hat{p}_i \sim \mathcal{U}(-0.2|\hat{p}_i|, 0.2|\hat{p}_i|)$$

The parameters related to physical constants are exempt. The errors in the parameters are kept constant throughout the growing season. Parameter uncertainty and weather forecast uncertainty is treated individually to better reveal their distinct effects.

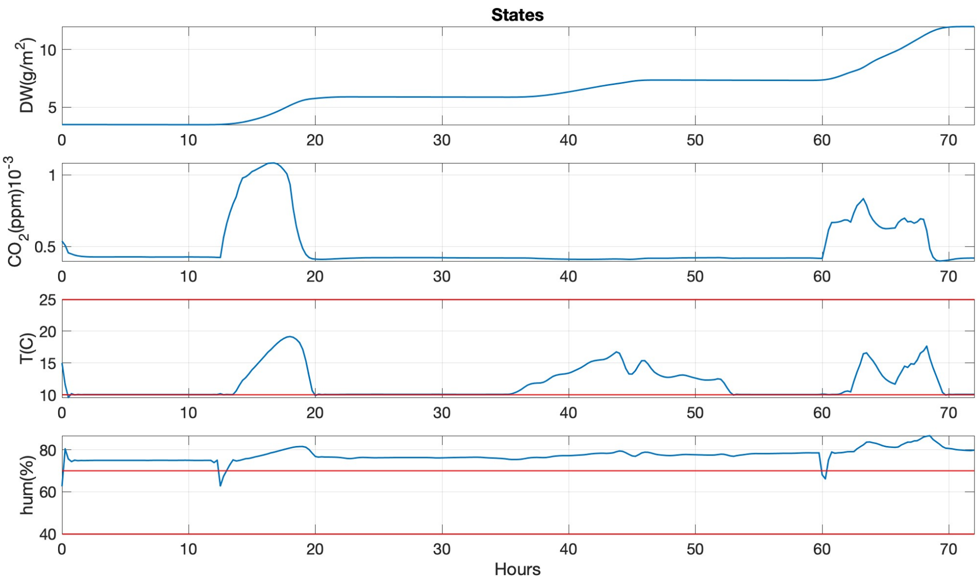

Figure 3-4: Simulation of the lettuce greenhouse controlled by NMPC with parameter error.

Chapter 4

SMPC Through System Linearization

Stochastic model predictive control or chance-constraied MPC entails the use of a probabilistic constraint in the following form.

$$\mathbb{P}(x_k \in \mathbb{X}_p) \geq 1 - \epsilon, \quad \forall k \tag{4-1}$$

To reformulate such a constraint as a deterministic constraint it is necessary to derive knowledge about the probability distribution of future states from the expected probability distribution of the uncertainty. Tracking the uncertainty propagation throughout the MPC horizon is a difficult problem discussed more in Section 2-3-2. It becomes much simpler for linear systems with Gaussian uncertainty where analytical solutions are available. This chapter discusses several SMPC formulations obtained through system linearization.

4-1 Linearizing Around a Point

The lettuce greenhouse model ($\frac{\mathrm{d}x}{\mathrm{d}t} = f(x, u, d, p)$, $y = g(x, p)$) can be linearized around a point in time such that:

$$\begin{aligned} \Delta x(t) &= x(t) - x(t_0), \quad & \Delta d(t) &= d(t) - d(t_0), \\ \Delta u(t) &= u(t) - u(t_0), \quad & \Delta p(t) &= p(t) - p(t_0), \end{aligned}$$

which results in the following linear system.

$$\begin{aligned} \frac{\mathrm{d}\Delta x(t)}{\mathrm{d}t} &= A_l \Delta x(t) + B_l \Delta u(t) + D_l \Delta d(t) + E_l \Delta p(t) \\ \Delta y(t) &= C_l \Delta x(t) \end{aligned}$$

$$\begin{aligned} A_l &:= \frac{\partial f}{\partial x}(x(t_0), u(t_0), d(t_0), p(t_0)), \quad & D_l &:= \frac{\partial f}{\partial d}(x(t_0), u(t_0), d(t_0), p(t_0)) \\ B_l &:= \frac{\partial f}{\partial u}(x(t_0), u(t_0), d(t_0), p(t_0)), \quad & E_l &:= \frac{\partial f}{\partial p}(x(t_0), u(t_0), d(t_0), p(t_0)) \\ C_l &:= \frac{\partial g}{\partial x}(x(t_0), p(t_0)) \end{aligned}$$

Finally, the model is discretized using a zero-order hold method resulting in the following.

$$\begin{aligned}\Delta x_{k+1} &= A\Delta x_k + B\Delta u_k + D\Delta d_k + E\Delta p_k \\ \Delta y_k &= C\Delta x_k\end{aligned}$$

The linearized and discretized system can be written as a single equation by vectorizing the variables such that $\mathbf{x} = \begin{bmatrix} x_0^T & x_1^T & \dots & x_N^T \end{bmatrix}^T$:

$$\begin{aligned}\Delta\mathbf{x} &= \mathbf{A}\Delta x_0 + \mathbf{B}\Delta\mathbf{u} + \mathbf{D}\Delta\mathbf{d} + \mathbf{E}\Delta\mathbf{p} \\ \Delta\mathbf{y} &= \mathbf{C}\Delta\mathbf{x}\end{aligned}$$

where,

$$\mathbf{A} := \begin{bmatrix} A^0 \\ A^1 \\ A^2 \\ \vdots \\ A^N \end{bmatrix}, \; \mathbf{T} := \begin{bmatrix} 0 & 0 & \cdots & 0 \\ I & 0 & \cdots & 0 \\ A & I & \ddots & \vdots \\ \vdots & \vdots & \ddots & 0 \\ A^{N-1} & A^{N-2} & \dots & I \end{bmatrix},$$

$$\mathbf{B} := \mathbf{T} \otimes B, \quad \mathbf{C} := I_N \otimes C, \quad \mathbf{D} := \mathbf{T} \otimes D, \quad \mathbf{E} := \mathbf{T} \otimes E.$$

The input-output constraints can now be expressed as the following.

$$\underbrace{\begin{bmatrix} \mathbf{y}(t_0) \\ -\mathbf{y}(t_0) \\ \mathbf{u}(t_0) \\ -\mathbf{u}(t_0) \end{bmatrix}}_{\mathbf{c}_0} + \underbrace{\begin{bmatrix} \mathbf{CA} \\ -\mathbf{CA} \\ 0 \\ 0 \end{bmatrix}}_{\mathbf{H}} x_0 + \underbrace{\begin{bmatrix} \mathbf{CB} \\ -\mathbf{CB} \\ I_{3N} \\ -I_{3N} \end{bmatrix}}_{\mathbf{F}} \Delta\mathbf{u} + \underbrace{\begin{bmatrix} \mathbf{CD} \\ -\mathbf{CD} \\ 0 \\ 0 \end{bmatrix}}_{\mathbf{G}_d} \Delta\mathbf{d} + \underbrace{\begin{bmatrix} \mathbf{CE} \\ -\mathbf{CE} \\ 0 \\ 0 \end{bmatrix}}_{\mathbf{G}_p} \Delta\mathbf{p} \leq \underbrace{\begin{bmatrix} \mathbf{y}_{\max} \\ -\mathbf{y}_{\min} \\ \mathbf{u}_{\max} \\ -\mathbf{u}_{\min} \end{bmatrix}}_{\mathbf{c}} \tag{4-2}$$

4-1-1 Constraint Tightening

The chance constraint can be reformulated as the following robust constraint where $\mathbf{w}$ represents the uncertain weather conditions $\Delta\mathbf{d}$ and model parameters $\Delta\mathbf{p}$.

$$\mathbf{G}\mathbf{w} \leq \mathbf{c} - \mathbf{c}_0 - \mathbf{H}\Delta x_0 - \mathbf{F}\Delta\mathbf{u}, \quad \forall\mathbf{w} \in \mathcal{W}. \tag{4-3}$$

The disturbance set $\mathcal{W}$ should be constructed to express the disturbance realizations that occur within a determined probability. It should also be formulated in a way that does not complicate the optimization problem. Two widely used formulations are polytopic sets (Equation 4-4) and norm-bounded sets (Equation 4-5).

$$\mathcal{W} = \{\mathbf{w} \mid S\mathbf{w} \leq h\} \tag{4-4}$$

$$\mathcal{W} = \{\mathbf{w} \mid \mathbf{w} = E\mathbf{d} + f, \; ||\mathbf{d}|| \leq 1\} \tag{4-5}$$

When the disturbance set is constructed to exlude realizations which are more extreme than a certain ratio of the cases using Polytopic sets the resulting set ends up more conservative as the bound is enforced on each disturbance dimension independently. Whereas in reality the probability of two extremal realizations occurring simultaneously will correspond to a smaller probability. Polytopic sets also require the introduction of dual variables in the optimization. On the other hand they can potentially be solved efficiently by linear programming, however such a program is not able to deal with a nonlinear cost function. Norm-bounded sets approximate the true probabilities more closely and require nonlinear optimization. Norm-bounded sets are used in this thesis, as they are less conservative and a nonlinear cost function is preferred in some formulations.

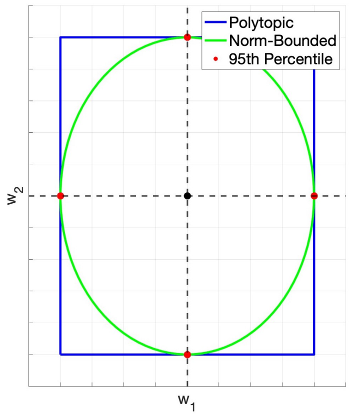

Figure 4-1: Bounds for a two dimensional 95th percentile disturbnace polytopic set and norm-bounded set.

The norm bounded disturbance set can be used to formulate a constraint exploiting the following relation which follows from the definition in Equation 4-5.

$$\max_{\mathbf{w}\in\mathcal{W}^N} a^T\mathbf{w} = ||E^T a|| + a^T f$$

Combining with Equation 4-3 the robust constraint becomes the following set of constraints where $(\cdot)_i$ refers to the i-th column.

$$||\mathbf{G}_i E|| + \mathbf{G}_i f \leq (\mathbf{c} - \mathbf{c}_0)_i - \mathbf{H}_i \Delta x_0 - \mathbf{F}_i \Delta \mathbf{u}, \quad \forall i$$

When the disturbance sequence is Gaussian with mean $\boldsymbol{\mu}$ and covariance $\boldsymbol{\Sigma}$, this corresponds to a constraint tightening of $||\mathbf{G}_i \boldsymbol{\Sigma}^{\frac{1}{2}}||\Phi^{-1}(1-\epsilon)$ and a shift of $\mathbf{G}_i\boldsymbol{\mu}$ on each row of the nominal linear constraints where Φ is the cumulative distribution function of the standard normal distribution. The estimated states will also be Gaussian when a linear model is used.

It is also possible to arrive at this constraint starting from the chance constraint in Equation 4-1 and defining $\mathbb{X}_p$ using Equation 4-2. The output sequence can be separated into a mean $\mathbf{y}_\mu = \mathbf{y}_0 + \mathbf{H}\Delta x_0 + \mathbf{F}\Delta\mathbf{u} + \mathbf{G}\boldsymbol{\mu}$ and a covariance $\boldsymbol{\Sigma}_y = \mathbf{G}\boldsymbol{\Sigma}\mathbf{G}^T$. Therefore the deviation from the mean for the i-th row of the output sequence will be below the following expression with probability $1-\epsilon$.

$$\sqrt{\mathbf{G}_i \boldsymbol{\Sigma} \mathbf{G}_i^T}\,\Phi^{-1}(1-\epsilon)$$

Both approaches result in the same constraint tightening which requires the system to stay within the constraints with probability $1-\epsilon$ at each time step. For linear systems with Gaussian uncertainty this is equivalent to ensuring complete constraint compliance under all but the most extreme disturbance realizations with probability ϵ at each time step. When the distribution is not Gaussian or is unknown, Chebyshev's inequality can provide an upper bound to the tightening by replacing $\Phi^{-1}(1-\epsilon)$ with $\sqrt{\frac{1}{\epsilon}}$ or with $\sqrt{\frac{1-\epsilon}{\epsilon}}$ when the mean is zero. This results in a more conservative constraint.

4-1-2 Linear SMPC

Linearizing the system around the most recent state and applying the constraint tightening as per the previous section leads to the following linear SMPC (LSMPC) scheme.

$$
\begin{aligned}
\min_{\Delta\mathbf{u},\mathbf{s}} \; & \mathbf{s}^T \boldsymbol{\lambda}\mathbf{s} + \sum_{k=0}^{N-1} -q_{p,2}(\Delta x_{\text{dw},k+1} - \Delta x_{\text{dw},k}) + \begin{bmatrix} q_{CO_2} & q_{vent} & q_{heat} \end{bmatrix} \Delta u_k \\
& \text{subject to} \\
& \Delta x_0 = \begin{bmatrix} 0 & 0 & 0 & 0 \end{bmatrix}^T \\
& \Delta\mathbf{d} \sim \mathcal{N}(\boldsymbol{\mu}, \boldsymbol{\Sigma}) \\
& \Delta x_{k+1} = A\Delta x_k + B\Delta u_k + D\mu_k, \quad \forall k \in \mathbb{I}_{[0:N-1]} \\
& ||\mathbf{G}_i \boldsymbol{\Sigma}^{\frac{1}{2}}||\Phi^{-1}(1-\epsilon) \leq (\mathbf{c}-\mathbf{c}_0)_i - \mathbf{F}_i\Delta\mathbf{u} - \mathbf{G}_i\boldsymbol{\mu} + \mathbf{s}, \quad \forall i \in \mathbb{I}_{[1:8(N+1)+6N]} \\
& -\frac{u_{\max}}{10} \leq \Delta u_k - \Delta u_{k-1} \leq \frac{u_{\max}}{10}, \quad \forall k \in \mathbb{I}_{[0:N-1]} \\
& \mathbf{s} \geq 0
\end{aligned}
\tag{4-6}
$$

Since the system is linearized around the current state, the initial state in the LRSMPC horizon is a vector of zeros. In the formulation given above parameter uncertainty is not present and the weather predictions have Gaussian uncertainty. For other distributions, Chebyshev's inequality can be resorted to as explained in at the end of the previous subsection. The cost represents the expected cost. The states are constrained to their expected values following the linear system dynamics and the probability distribution of the weather conditions. The original input-output constraints are tightened according to the variance of the weather forecasts. Finally, constraints were placed on the change in input such that the difference between each time step is smaller than or equal to a tenth of the input range. Without this constraint the scheme has been observed behave erratically with aggressive changes in inputs.

The cost function and the constraints in the optimization problem are both linear with respect to the inputs. The problem can therefore be solved simply by linear programming. This simplicity comes at the cost of linearization errors. Moreover, there is no structure in the control policy that allows it to react to disturbances in the prediction horizon. This is discussed more in Section 2-3-1. Such a structure can be introduced by adding an analytically calculated stabilizing state feedback gain to the input. This was attempted using gains calculated with the discrete Riccati equation, but these gains resulted in slower calculations and worse performance, instead of any improvements. Another way to achieve a feedback policy is to parametrize the input as a disturbance feedback such that $\Delta\mathbf{u} = \mathbf{M}\mathbf{w} + \mathbf{v}$ which introduces the matrix $\mathbf{M}$ into the optimization variables increasing the order of the number of variables. It also introduces $\mathbf{M}$ into the norm in the constraints complicating the optimization problem. Introducing the disturbance feedback parametrization was attempted, but it was abandoned after deciding that the added complexity was not justified by the expected benefits.

4-2 Linearizing Along a Trajectory

Linearizing the system introduces errors which grow as the states move away from the linearization point. Even when the states of the greenhouse stay close to the linarization, the weather conditions are bound to change. The effects of the ventilation input, for example, are highly dependent on the weather conditions. The LSMPC will erroneously expect the ventilation to have the same effect as it does at the current time throughout the prediction horizon. The controller will also be mostly blind to the effects of photosynthesis until sunrise. These can be alleviated by linearizing the system around the forecasted weather conditions to obtain a linear time-varying (LTV) system model. Moreover, the states can also be linearized around a trajectory instead of a single point.

$$\Delta x_k = x_k - \bar{x}_k, \quad \Delta d_k = d_k - \bar{d}_k,$$
$$\Delta u_k = u_k - \bar{u}_k, \quad \Delta p_k = p_k - \bar{p}_k,$$

The trajectory which solves the NMPC in Equation 3-2 constitutes a likely trajectory which is close to optimal. The NMPC can be solved to obtain a trajectory $(\bar{\mathbf{x}}, \bar{\mathbf{u}}, \bar{\mathbf{d}}, \bar{\mathbf{p}},)$ to linearize around.

$$\begin{aligned} A_k &:= \frac{\partial f}{\partial x}(\bar{x}_k, \bar{u}_k, \bar{d}_k, \bar{p}_k), \quad & D_k &:= \frac{\partial f}{\partial d}(\bar{x}_k, \bar{u}_k, \bar{d}_k, \bar{p}_k) \\ B_k &:= \frac{\partial f}{\partial u}(\bar{x}_k, \bar{u}_k, \bar{d}_k, \bar{p}_k), \quad & E_k &:= \frac{\partial f}{\partial p}(\bar{x}_k, \bar{u}_k, \bar{d}_k, \bar{p}_k) \\ C_k &:= \frac{\partial g}{\partial x}(\bar{x}_k, \bar{p}_k) \end{aligned}$$

The LTV system now becomes the following.

$$\begin{aligned} x_{k+1} &= A_k \Delta x_k + B_k \Delta u_k + D_k \Delta d_k + E_k \Delta p_k \\ \Delta y_k &= C_k \Delta x_k \end{aligned}$$

Expressed in a single equation the sequence of states is given by:

$$\begin{aligned} \Delta \mathbf{x} &= \mathbf{A}' \Delta x_0 + \mathbf{B}' \Delta \mathbf{u} + \mathbf{D}' \Delta \mathbf{d} + \mathbf{E}' \Delta \mathbf{p} \\ \Delta \mathbf{y} &= \mathbf{C}' \Delta \mathbf{x} \end{aligned}$$

where,

$$\mathbf{A}' := \begin{bmatrix} I \\ A_0 \\ A_1 A_0 \\ \vdots \\ A_{N-1} \dots A_1 A_0 \end{bmatrix}, \ \mathbf{T}' := \begin{bmatrix} 0 & 0 & \cdots & 0 \\ T_0 & 0 & \cdots & 0 \\ A_1 T_0 & T_1 & \ddots & \vdots \\ \vdots & \vdots & \ddots & 0 \\ A_{N-1} \dots A_1 T_0 & A_{N-2} \dots A_2 T_1 & \cdots & T_{N-1} \end{bmatrix};$$

for $T \in \{B, D, E\}$ and finally $\mathbf{C}'$ is a block diagonal matrix with the matrices $C_0, C_1, \dots, C_N$ on the diagonal.

4-2-1 Linear Time-Varying SMPC

Replacement of the linear system used in the LSMPC with the LTV system results in the following LTVSMPC scheme.

$$
\begin{aligned}
\min_{\Delta \mathbf{u},\mathbf{s}} \; & \mathbf{s}^T \boldsymbol{\lambda} \mathbf{s} + \sum_{k=0}^{N-1} -q_{p,2}(\Delta x_{\mathrm{dw},k+1} - \Delta x_{\mathrm{dw},k}) + \begin{bmatrix} q_{CO_2} & q_{vent} & q_{heat} \end{bmatrix} \Delta u_k \\
& \text{subject to} \\
& \Delta x_0 = \begin{bmatrix} 0 & 0 & 0 & 0 \end{bmatrix}^T \\
& \Delta \mathbf{d} \sim \mathcal{N}(0, \boldsymbol{\Sigma}) \\
& \Delta x_{k+1} = A_k \Delta x_k + B_k \Delta u_k, \quad \forall k \in \mathbb{I}_{[0:N-1]} \\
& ||\mathbf{G}_i' \boldsymbol{\Sigma}^{\frac{1}{2}}|| \Phi^{-1}(1-\epsilon) \leq (\mathbf{c} - \bar{\mathbf{c}})_i - \mathbf{F}_i' \Delta \mathbf{u} + \mathbf{s}, \quad \forall i \in \mathbb{I}_{[1:8(N+1)+6N]} \\
& -\frac{u_{\max}}{10} \leq \Delta u_k - \Delta u_{k-1} \leq \frac{u_{\max}}{10}, \quad \forall k \in \mathbb{I}_{[0:N-1]} \\
& \mathbf{s} \geq 0
\end{aligned}
\tag{4-7}
$$

The scheme relies on the trajectory obtained by the NMPC and can be seen as a stochastic correction on top of it. Since the dynamics of the system are linearized around the mean prediction, the uncertainty in the LTVSMPC has zero mean. An outline of the scheme is presented in Algorithm 1. It is possible to use the nonlinear dynamics in the evolution of the states in Equation 4-7 for a more accurate cost representation. In this case, the scheme corresponds to solving the NMPC, then using the solution to construct a tightened constraint for an otherwise identical optimization problem. The version of the scheme with a nonlinear cost will be referred to as the NSMPC, its exact formulation is given in Equation 4-8.

$$
\begin{aligned}
\min_{\Delta \mathbf{u},\mathbf{s}} \; & \mathbf{s}^T \boldsymbol{\lambda} \mathbf{s} + \sum_{k=0}^{N-1} -q_{p,2}(x_{\mathrm{dw},k+1} - x_{\mathrm{dw},k}) + \begin{bmatrix} q_{CO_2} & q_{vent} & q_{heat} \end{bmatrix} \Delta u_k \\
& \text{subject to} \\
& x_0 = x \\
& \mathbf{d} \sim \mathcal{N}(\boldsymbol{\mu}, \boldsymbol{\Sigma}) \\
& x_{k+1} = f_d(x_k, \bar{u}_k + \Delta u_k, \mu_k), \quad \forall k \in \mathbb{I}_{[0:N-1]} \\
& ||\mathbf{G}_i' \boldsymbol{\Sigma}^{\frac{1}{2}}|| \Phi^{-1}(1-\epsilon) \leq (\mathbf{c} - \bar{\mathbf{c}})_i - \mathbf{F}_i' \Delta \mathbf{u} + \mathbf{s}, \quad \forall i \in \mathbb{I}_{[1:8(N+1)+6N]} \\
& -\frac{u_{\max}}{10} \leq \Delta u_k - \Delta u_{k-1} \leq \frac{u_{\max}}{10}, \quad \forall k \in \mathbb{I}_{[0:N-1]} \\
& \mathbf{s} \geq 0
\end{aligned}
\tag{4-8}
$$

When the inputs are zero, the LTVSMPC and the NSMPC will follow the NMPC. They will deviate from this trajectory in order to satisfy the stochastic constraints which mandate a safe distance from the nominal constraints. If the cost was defined as the distance from the NMPC trajectory, this would be the only cause of deviation. However, with the economic cost, they may also deviate if this deviation results in a lower cost in the prediction horizon. In a different application, a quadratic cost on deviation from the predetermined trajectory may be the preferable cost.

Algorithm 1 LTVSMPC

1: **Inputs:** Initial state x and input u^{-}, predictions for the uncertain variables $(\boldsymbol{\mu}, \boldsymbol{\Sigma})$.
2: **Solve:** NMPC with x,u^{-},$\boldsymbol{\mu}$ (Equation 3-2).
3: **Construct:** SMPC with Δu^{-} and $\boldsymbol{\Sigma}$, linearized around the trajectory obtained from the NMPC.
4: **Solve:** Linearized SMPC (Equation 4-7).
5: **Outputs:** The initial control action u_0, from the solutions of second and fourth steps.

Chapter 5

SMPC with Adaptive Constraints

The previous chapter discusses analytic controllers which are built according to the available knowledge about the system and the present uncertainties. However, such a controller cannot adjust itself based on the knowledge gained during operation. If the controller is too conservative hurting the cost, or is not conservative enough and leading to excessive constraint violations, it will not be able to adapt to these observations. Since the distribution of weather forecast error and parameter error also contains uncertainty, and since linearization also introduces errors, it is expected that these controllers contain bias in one direction or the other. To overcome this problem, it is necessary to incorporate on-line information into the control scheme. This chapter discusses a simple but effective way to achieve this.

SMPC can be formulated with adaptive constraints [46]. One way to formulate such constraints is through the notion of average constraint violations [31] (Section 2-3-2):

$$\frac{\hat{v}_{t+1}}{\tau_{t+1}} \leq \xi, \tag{5-1}$$

where v and s respectively represent the decaying total observed violation and the decaying total time with decay rate $\gamma \in [0, 1]$, they are defined below where $l(\cdot)$ returns a vector of the amount of constraint violation for each constraint that is included in the adaptive tightening or 0 for ones that are excluded.

$$v_t := \sum_{k=0}^{t} \gamma^{t-k} l(x_t), \quad t \in \mathbb{I}_{\geq 0}$$

$$\tau_t := \sum_{k=0}^{t} \gamma^{t-k}, \quad t \in \mathbb{I}_{\geq 0}$$

It is also possible to only count the violations and disregard the amount by which each constraint is violated. This would be more consistent with the goal of ensuring constraint compliance with a certain probability. Using the average violation, on the other hand, acts similar to the CVaR constraints in Section 2-3-2 in the sense that they punish not only constraint violations, but also the amount by which the constraints are violated. The average violation constraints are preferred in this thesis for this desirable effect and also to avoid introducing integer variables into the optimization problem.

5-1 Adaptive Constraint Tightening

The average constraint violation constraint in Equation 5-1 can be expressed in terms of the next state as follows.

$$\xi\tau_{s+1} - v_{t+1} = \xi\tau_{t+1} - \gamma v_t - l(x_{t+1}) \geq 0$$

$$l(x_{t+1}) \leq \gamma(\xi\tau_t - v_t) + \xi$$

This can then be used to constrain an estimate of the next state, for linear systems, the expected value of the next state can be used as the estimate.

$$\begin{bmatrix} \max\{g(f_d(x_t, u_t, \hat{d}_t, \hat{p}), \hat{p}) - y_{\max},\, 0\} \\ \max\{-g(f_d(x_t, u_t, \hat{d}_t, \hat{p}), \hat{p}) + y_{\min},\, 0\} \end{bmatrix} \leq \gamma(\xi\tau_t - v_t) + \xi$$

This constraint is adaptive in the sense that it will react to the empirical violations. The constraint becomes tighter when the observed violation is above the decaying average violation up until it reaches ξ and becomes more relaxed when the observed violation is below the current decaying average. The expectation is for this constraint to act like an integrator and for the empirical average violations to eventually settle around the prescribed limit. For it to be possible to satisfy this constraint, the right-hand side of the inequality has to be nonnegative. This can be forced by modifying the bound as follows, where β is a non-negative upper bound on the maximum allowable violation.

$$\max\{\gamma(\xi\tau_t - v_t) + \xi,\, \beta\}$$

Now, the maximums on the left side can be removed as the new constraint is trivially satisfied when $\max\{\cdot,\, 0\} = 0$. Another effect of this modification is that it is no longer possible for this constraint to tighten the original constraints $y_{\min} \leq g(x) \leq y_{\max}$, but only to relax them.

It is possible to combine a version of this constraint with another constraint that decides the initial tightening. In fact, adaptive constraints were initially considered only to reduce the conservatism of the controllers described in the previous chapter. However, if the other tightening method results in significantly different constraints between time steps, this may inhibit the convergence of the adaptive constraint, as it would also have to adapt to this additional constraint. In this thesis, the average violation constraint will be employed alongside an extreme static constraint tightening α which is chosen such that it tightens the temperature constraints by 5°C, the relative humidity constraints by 25% and sets the remaining constraints to their nominal values. The maximum deviation allowed for any time step is chosen as ±1°C for the temperature and ±5% for the relative humidity, i.e., the amount of violation which would lead to the tightest possible constraints even if the average violation were zero just before. ξ is chosen as this maximum violation multiplied by the acceptable probability of violation ϵ. The resulting constraints can be understood as allowing for the maximum violation with probability ϵ, allowing for ϵ times the maximum violation at each time step, and everything in between, as long as it results in an equivalent decaying average. Since ξ indirectly accounts for the maximum violations, β is chosen to equal a vector of zeros.

$$\begin{bmatrix} g(f_d(x_t, u_t, d_t, \hat{p}), \hat{p}) - y_{max} \\ -g(f_d(x_t, u_t, d_t, \hat{p}), \hat{p}) + y_{min} \end{bmatrix} \leq \max\{\gamma(\xi\tau_t - v_t) + \xi,\, 0\} - \alpha$$

When the decay rate is equal to one, all past violations will effect the constraint equally and the constraint can be relaxed indefinitely if no violations are observed. When the decay rate factor is smaller than one, the decaying total time is bounded $s_\infty = (1-\gamma)^{-1}$. This is preferable because an unbounded total time can build up allowing for a lot of violation before it has a significant effect on the average and before the controller can meaningfully adapt. Moreover, more distant violations will have a smaller effect on the average when a decay rate is present.

The decay rate is chosen such that $\tau_\infty = 2\alpha/\xi$. The resulting constraint can tighten or relax the original constraints roughly by α, when the average violation is 0 the right-hand side of the constraint is $(2\gamma - 1)\alpha + \xi$ and it is -α when the average violations are above ξ. If τ is initialized at $\tau_\infty/2$, the constraint for the initial time step will be equivalent to the original constraints. An undesirable consequence of allowing constraint relaxation is that the scheme will always result in some violation as long as the local minimum is outside the constraints. In applications similar to the greenhouse, where the operating on the constraints is often optimal and small violations can be tolerated, this may indeed be desirable. Otherwise, the static tightening may be chosen such that $\alpha = \xi\tau_\infty$ which would not allow the constraints to relax beyond their original value and, therefore, would not cause the same unnecessary violations. Both choices for the static tightening are investigated in the simulations.

5-2 Adaptive SMPC

Introducing the decaying total violation v as a variable in the optimization problem would be ideal, however, this results in a constraint that depends on the maximum between a variable and a scalar, which significantly increases the computational demands. On the other hand, if it is updated after measurements and kept constant in the MPC horizon it causes no additional demands and acts as a static tightening on the constraints. The downside is that now, the optimization problem is blind to the dynamics of the adaptive constraint. Still, the cost of this blindness will become more limited as the average violation converges.

$$
\begin{aligned}
\min_{\mathbf{u}} \ \mathbf{s}^T \boldsymbol{\lambda} \mathbf{s} + \sum_{k=0}^{N-1} -q_{p,2}(x_{\mathrm{dw},k+1} - x_{\mathrm{dw},k}) + \begin{bmatrix} q_{CO_2} & q_{vent} & q_{heat} \end{bmatrix} u_k \\
\text{subject to} \\
x_0 &= x \\
x_{k+1} &= f_d(x_k, u_k, \hat{d}_k, \hat{p}), \quad \forall k \in \mathbb{I}_{[0:N-1]} \\
\begin{bmatrix} g(x_{k+1}, \hat{p}) - y_{max} \\ -g(x_{k+1}, \hat{p}) + y_{min} \end{bmatrix} &\leq \max\{\gamma(\xi\tau_t - v_t) + \xi,\, 0\} - \alpha + \mathbf{s}, \quad \forall k \in \mathbb{I}_{[0:N-1]} \\
u_{\min} &\leq u_k \leq u_{\max}, \quad \forall k \in \mathbb{I}_{[0:N-1]} \\
-\frac{u_{\max}}{10} &\leq u_k - u_{k-1} \leq \frac{u_{\max}}{10}, \quad \forall k \in \mathbb{I}_{[0:N-1]} \\
\mathbf{s} &\geq 0
\end{aligned}
\tag{5-2}
$$

After a measurement v and s are updated according to their previous values. It is also possible to directly calculate τ from the value of t.

$$\begin{aligned} v_t &= \gamma v_{t-1} + \begin{bmatrix} \max\{g(x_t, p) - y_{max},\, 0\} \\ \max\{-g(x_t, p) + y_{min},\, 0\} \end{bmatrix} \\ \tau_t &= \gamma \tau_t + 1 \end{aligned}$$

This adaptive SMPC (ASMPC) scheme is remarkable because it can quickly adapt to both stochastic uncertainties and unseen model biases. If the underlying system is deterministic it will be easier for the constraints to converge. However, they can also adapt to an underlying independent and identically distributed disturbance. Therefore, the scheme does not require information about the underlying uncertainties, only that they be sufficiently small and regular. It leverages the efficiency of simply setting a heuristic safety margin in the face of uncertainty. The formulation ends up relatively simple by focusing directly on the empirical constraint violation, the very thing that is to be controlled. This simplicity allows the constraint tightening to potentially be used alongside other methods without much trouble in implementation.

Chapter 6

Simulation Results & Discussion

Real-life weather data is taken from Kempkes et al.[29] collected from 'the Venlow Energy greenhouse', located in Bleiswijk, with a sample period of 5 minutes. It is resampled at a sampling time of 15 minutes. A growth period of 28 days is considered. All controllers were constructed with a prediction horizon of 6 hours. Everything else related to the formulation of the simulations is presented in Section 2-1 and Chapter 3. In order to reach statistical significance, 30 growth cycles were simulated with different uncertainty realizations independently for both weather forecast and parameter uncertainty. The source code and simulation results can be found at https://github.com/UmutSelcuk/SMPCGreenhouse. The plots for the weather data and for some of the simulated scenarios are given in Appendix A.

All optimization problems for the controllers were solved with the open-source software CasADi from Andersson et al.[2] and the solver IPOPT by Wächter and Biegler [65] in a MATLAB environment. All optimization problems were warm started from the previous solutions except the LTVSMPC and NSMPC which are already linearized around a close-to-optimal trajectory. The control schemes considered are summarized below.

- **NMPC/IMPC:** A simple nonlinear model predictive control scheme as described in Equation 3-2. IMPC is a version of the same controller with access to perfect model parameters and weather forecast to act as an ideal.
- **LSMPC(W/P):** A linear stochastic model predictive control scheme obtained analytically through system linearization around the current states, described in Section 4-1-2. Has full knowledge of the probability distribution of the uncertainties. The formulation is different for parametric uncertainty and weather forecast uncertainty.
- **LTVSMPC/NSMPC(W/P)** Similar to LSMPC, but linearized around a trajectory obtained through the NMPC. NSMPC is a version of the LTVSMPC that uses a nonlinear cost, both are described in Section 4-2-1.
- **ASMPC/SASMPC** An adaptive stochastic model predictive control scheme which relies on tracking the average empirical constraint violations to shift the constraints

on the NMPC, described in Section 5-2. SAMPC or safe AMPC is a version of the ASMPC with a static constraint tightening such that it can only tighten constraints and cannot relax them. The formulation of these schemes is independent of the uncertainty considered.

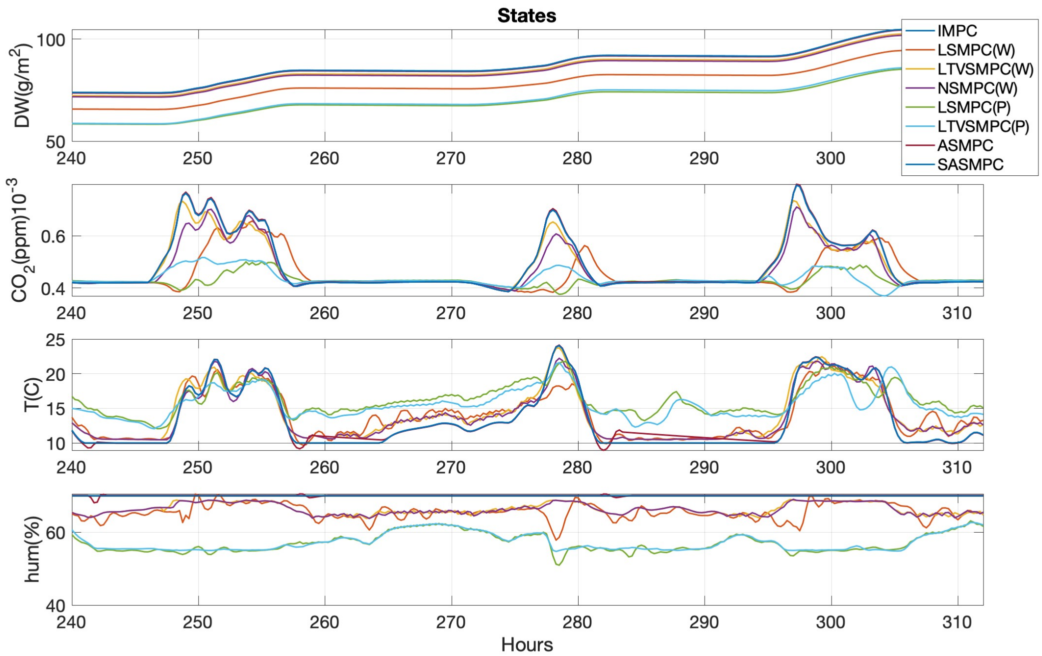

Figure 6-1: 3-Day period in the middle of a growth-cycle as controlled by all mentioned schemes in a simulation with no uncertainty.

The states when controlled by the mentioned controllers when no uncertainty is present are plotted in Figure 6-1, the corresponding control inputs are shown in Figure 6-2. Compared to the NMPC, which is equivalent to IMPC in this case, the linearized stochastic schemes for parametric uncertainty result in a considerable decrease in the profit (Equation 2-2) of around 32.5% at the end of the growth cycle. A major factor in these losses is the excessive heating applied to keep temperatures well above the lower bound at nighttime. The LTVSMPC and NSMPC when formulated for weather forecast uncertainty, decreased profits by around 8.5%, the LSMPC was more costly leading to a decrease of 11.9%. The linearized schemes also lead to more erratic inputs compared to the other controllers which have smooth input trajectories. The adaptive schemes are much less conservative. The SASMPC results in a decrease less than 1% and the ASMPC leads to a minute increase in profit. This increase is due to the nature of the ASMPC, as it requires a small amount of violation (0.5ξ) to maintain the decaying average constraint violation. It also relaxes the constraints whenever the violation observed is below this value, and steers back if this leads to more violation. These small violations and constraint relaxations, which are not permitted for any of the other controllers, are the cause for the increase in profit. The same effect causes constraint violations when the temperature reaches the lower bound each night, this is then corrected after some violation is observed. The only other controller that caused any violations when no uncertainty is present is the LSMPC, presumably due to linearization error.

The nominal case reveals some insights about the "reasoning" of the controllers. One such insight is related to the effect of the day-night cycle on the analytical constraint tightening. The schemes which were formulated to deal with weather forecast uncertainty apply more tightening during the night which is consistent with the fact that a drop in temperature leads to an increase in the relative humidity. When formulated for parametric uncertainty, there is significantly more tightening and this effect is reversed. This is likely caused by the effect of photosynthesis which is absent at night and may be significantly impacted by parametric uncertainty, therefore increasing the total uncertainty during the day. This is supported by the fact that this effect becomes more pronounced as the plant grows. These schemes are also more reluctant to inject carbon dioxide into the system. Their preference for a high ventilation to keep the humidity low devalues carbon dioxide injection. The LSMPC additionally suffers from blindness, as when the system is linearized a point, it cannot adequately benefit from forecasts. Consequently, it remains idle as the other schemes increase carbon dioxide in anticipation of sunlight, reacts only after the first light, and is late to turn it off for sunset.

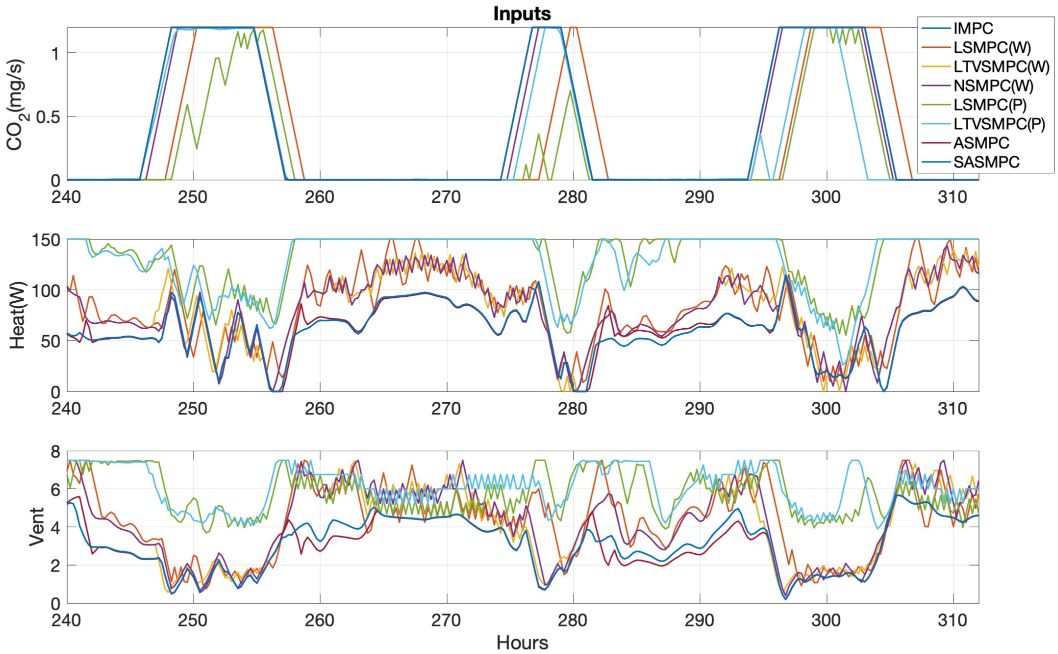

Figure 6-2: Control inputs for a 3-Day period in the middle of a growth-cycle as controlled by all mentioned schemes in a simulation with no uncertainty.

6-1 Weather Forecast Uncertainty

30 simulations are performed under each control scheme for different weather forecast uncertainty realizations. The results are tabulated in Table 6-1.

6-1-1 Constraint Violations

The linearized schemes were able to meet their goal and keep the overall violation rate below 5%, i.e., less than five percent of the time steps were spent outside of the constraints. The adaptive schemes, which were indirectly formulated for the same goal, resulted in a small excess over this goal, but the average violations were significantly below the actual constraint that was imposed. The SASMPC resulted in a lower violation rate compared to the ASMPC. Overall, the violation rate of the stochastic controllers are similar and they eliminate more than 90% of the time the NMPC controlled system spends under violation.

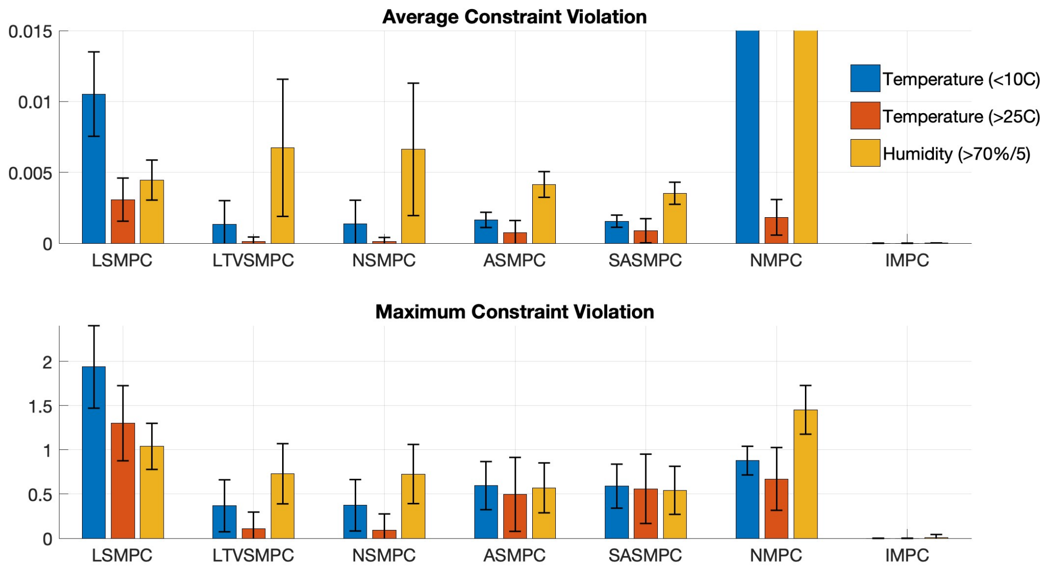

Figure 6-3: Mean and standard deviation of the average constraint violation and maximum constraint violation observed over 30 simulations of a 28 day growth period with different weather forecast error realizations, for each controller.

The LTVSMPC and the NSMPC performace is quite similar. Comparatively, the LSMPC resulted in a lower rate of violation, but also in significantly higher average temperature violations and maximum violations, even higher than the NMPC for some of them. The maximum and average violations are plotted in Figure 6-3. All other schemes resulted in a decrease in the average and maximum violations. The adaptive schemes were better at constraining the humidity violations and the linearized schemes were better at controlling the temperature. This difference is rooted in the difference in the weighing of the constraint violations in humidity and temperature in the adaptive schemes. The adaptive schemes are also expected to result in more temperature violations as the optimal trajectory often moves away from constraint boundaries unlike the humidity.

6-1-2 Costs

Improved constraint compliance comes at an economic cost. The costs related to each cotroller is plotted in Figure 6-4. Even the IMPC is associated with a higher cost compared to the NMPC. The LSMPC resulted in the highest cost and the lowest increase in plant mass. This conservativity is not well justified as the LTVSMPC and NSMPC lead to both lower average and maximum constraint violations, and a higher profit. They do result in a bigger increase in the input costs which are made up by the higher yield. This difference is due to the LSMPC failing to properly use the CO_2 input. Between the two, the NSMPC prefers lower input costs and a reduction in yield, in terms of profit these differences even out and the performance is very similar overall. The NSMPC is more computationally expensive due to its nonlinear formulation. The LSMPC and the LTVSMPC are similar and the extra NMPC solved for the LTVSMPC has a minimal impact on the computation time, the linear optimization problem is easier to solve when initialized around an optimal trajectory which compensates for some of the additional computation time incurred by solving two problems instead of one.

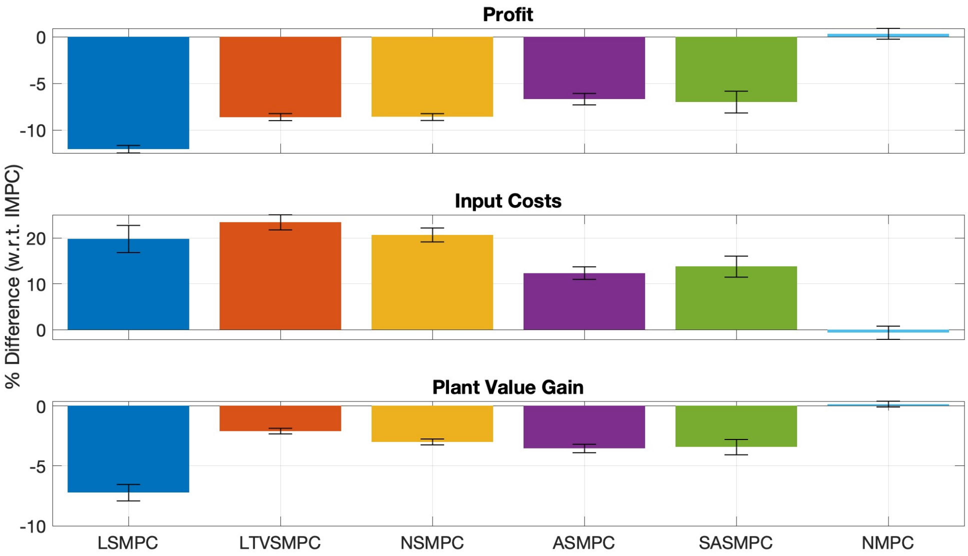

Figure 6-4: Mean and standard deviation of the percentage difference in economic profit, total input costs and the economic value of the increase in plant mass over 30 simulations of a 28 day growth period with different weather forecast error realizations, for each controller.

The adaptive schemes resulted in the lowest reduction in profit and the lowest input costs out of all the stochastic controllers. They do result in a lower yield that is more than compensated for by the lower input costs. This is notable as performance was comparable across most control schemes in terms of constraint compliance. Moreover, they are computationally cheaper compared to the other schemes as their related optimization problem is equivalent to the NMPC in terms of complexity. The SASMPC results in a slightly higher cost with a higher variance and marginally lower constraint violations. The difference in violations is less defined compared to the case with no disturbances where the SASMPC results in no violation at all. Shorter computation times compared to the ASMPC and the NMPC may be due to this reduction in violations.

Table 6-1: Controller performance under weather uncertainty.

	LSMPC		**LTVSMPC**		**NSMPC**		**ASMPC**		**SASMPC**		**NMPC**	
	μ	σ	μ	σ	μ	σ	μ	σ	μ	σ	μ	σ
Constraint Violations												
Rate (%)	3.677	0.559	4.605	1.856	4.512	1.834	6.011	0.572	5.396	0.421	65.435	7.771
Average ($\times10^{-2}$)												
Temperature (< 10°C)	1.052	0.298	0.134	0.166	0.137	0.167	0.165	0.054	0.156	0.043	3.283	0.786
Temperature (> 25°C)	0.308	0.152	0.014	0.030	0.012	0.029	0.075	0.085	0.088	0.085	0.183	0.126
Humidity (> 70%)	2.227	0.706	3.365	2.420	3.310	2.336	2.073	0.453	1.763	0.390	69.51	14.81
Maximum												
Temperature (< 10°C)	1.937	0.466	0.367	0.294	0.373	0.291	0.595	0.272	0.590	0.249	0.878	0.162
Temperature (> 25°C)	1.301	0.425	0.106	0.191	0.092	0.183	0.496	0.418	0.559	0.392	0.671	0.355
Humidity (> 70%)	5.194	1.303	3.648	1.702	3.633	1.671	2.850	1.411	2.710	1.359	7.260	1.377
Costs Compared to IMPC(Δ%)												
Profit	-12.07	0.407	-8.619	0.380	-8.612	0.370	-6.688	0.615	-7.003	1.170	0.341	0.579
Input Costs	19.79	2.960	23.42	1.647	20.67	1.519	12.35	1.371	13.76	2.292	-0.666	1.444
Growth Value	-7.238	0.685	-2.102	0.234	-3.005	0.247	-3.551	0.351	-3.439	0.638	0.152	0.239
Computation Time (s)												
Average	1.219	0.164	1.458	0.143	1.796	0.229	0.433	0.061	0.273	0.026	0.450	0.063
Maximum	5.097	1.366	4.603	1.936	5.859	0.844	6.773	1.046	2.791	0.281	3.183	0.637

Table 6-2: Controller performance under parameter uncertainty.

	LSMPC		**LTVSMPC**		**ASMPC**		**SASMPC**		**NMPC**		**IMPC**	
	μ	σ	μ	σ	μ	σ	μ	σ	μ	σ	μ	σ
Constraint Violations												
Rate (%)	9.072	16.04	7.771	15.71	83.54	11.14	15.61	24.81	63.94	47.83	61.04	16.18
Average ($\times10^{-1}$)												
Temperature (< 10°C)	0.022	0.051	0.058	0.124	0.156	0.075	0.065	0.275	0.143	0.196	0.205	1.125
Temperature (> 25°C)	0.531	0.521	0.095	0.096	0.148	0.118	0.158	0.212	0.044	0.074	0.001	0.002
Humidity (> 70%)	2.214	7.704	1.919	7.803	8.624	22.96	10.68	44.63	31.64	41.74	1.590	6.903
Maximum												
Temperature (< 10°C)	0.747	0.363	0.573	0.595	1.098	0.197	0.414	0.732	0.185	0.193	0.065	0.354
Temperature (> 25°C)	6.018	5.247	1.687	1.326	2.053	0.697	1.798	1.929	0.520	0.542	0.005	0.018
Humidity (> 70%)	6.474	3.738	2.644	4.063	5.631	4.343	6.027	9.557	7.096	8.831	2.267	3.167
Costs Compared to IMPC(Δ%)												
Profit	-32.47	8.245	-31.54	11.46	-7.978	8.661	-0.456	29.16	1.672	15.33	0.000	0.000
Input Costs	60.80	29.10	69.34	40.09	8.147	12.60	8.833	60.97	7.256	39.78	0.000	0.000
Growth Value	-16.52	7.585	-13.67	10.85	-4.355	5.395	0.565	17.08	1.747	13.78	0.000	0.000
Computation Time (s)												
Average	1.277	0.239	1.424	0.131	0.251	0.023	0.275	0.033	0.294	0.027	0.257	0.026
Maximum	4.697	1.094	3.823	0.666	1.512	0.241	2.022	0.979	1.665	0.229	1.474	0.450

6-2 Parameter Uncertainty

30 simulations are performed under each control scheme for different parameter uncertainty realizations. The NSMPC is omitted as it resulted in significantly higher computational demands compared to the weather uncertainty case. The results are tabulated in Table 6-2.

6-2-1 Constraint Violations

The variances for most observations are significantly higher compared to the case with weather uncertainty. This is a consequence of the parameters staying constant throughout the growth cycle. Unlike the case with weather forecast uncertainty, none of the control schemes were able to attain a constraint violation rate below 5% in the presence of parametric uncertainty. The adaptive schemes also failed to meet their average violation constraints on humidity. However, it should be noted that even the IMPC resulted in a violation rate of 6%. This time around, the LTVSMPC resulted in the lowest violation rate with a slightly lower variance than the IMPC. The ASMPC resulted in a violation rate higher than even the NSMPC. The SASMPC, on the other hand, did significantly decrease the violation rate even if it fell short in this regard compared to the linearized controllers. The LTVSMPC resulted in the lowest average and maximum violations as shown in Figure 6-5, while the LSMPC performed considerably worse, especially in the temperature and the maximum violations.

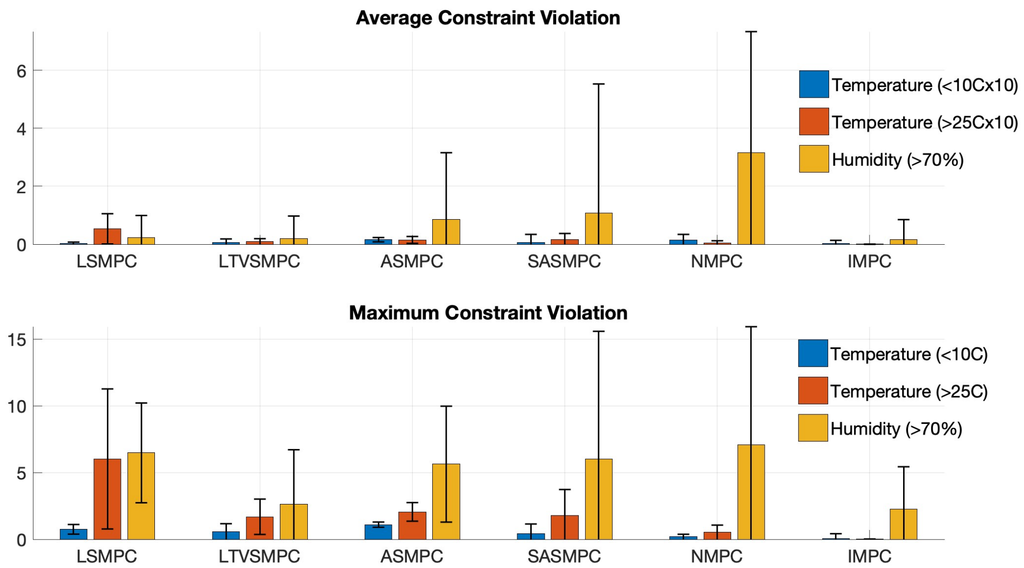

Figure 6-5: Mean and standard deviation of the average constraint violation and maximum constraint violation observed over 30 simulations of a 28 day growth period with different parameter realizations, for each controller.

The adaptive schemes resulted in higher average and maximum constraint violations compared to the LTVSMPC. The difference between the adaptive schemes are more pronounced under parameter uncertainty. The constraint violations were comparable with the ASMPC showing better performance in humidity and worse in temperature. The variance of the SASMPC performance was significantly higher. Though at a much lower rate, the violations of the SASMPC can be considerably higher than the ASMPC. As it results in violations less often, it may require more time before the constraints can meaningfully adapt when the violations eventually do materialize, leading to higher violations in the meantime.

6-2-2 Costs

The linear controllers end up very costly similar to the case with no disturbance causing more than 30% reduction in profits compared to IMPC. The LTVSMPC results in higher input costs and a higher yield compared to the LSMPC, which fails to optimally exploit the CO_2 input, and is slightly more profitable. It also has a higher variance in these costs. The conservativity in the linearized schemes lead to a serious increase in input costs of more than 60%. The computation times were similar to the weather uncertainty case. Notably, the NSMPC had significantly higher computation times, enough to make it impractical in the simulation study, especially considering how close its results were to the LTVSMPC under weather uncertainty and in the small amount of simulations performed with parametric uncertainty.

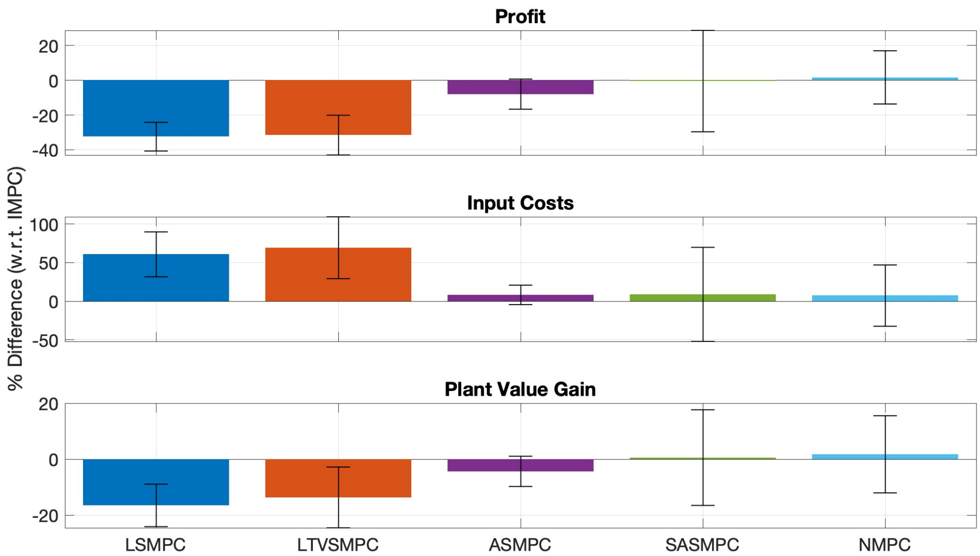

Figure 6-6: Mean and standard deviation of the percentage difference in economic profit, total input costs and the economic value of the increase in plant mass over 30 simulations of a 28 day growth period with different parameter realizations, for each controller.

The ASMPC resulted in a much more acceptable reduction in profit and the SASMPC resulted in almost no reduction at all. Although, the costs associated with the SASMPC have a starkly higher variance. Since it cannot relax the constraints, the SASMPC owes its low cost to the violations it results in. The ASMPC can increase profits by relaxing the constraints, but results show a loss on average. The costs related with the ASMPC have markedly low variance. It also has somewhat lower input costs compared to the SASMPC, both of which are remarkably close to the input costs of the NMPC.

6-2-3 Results without Extreme Cases

In 14 of the 30 cases considered for parametric uncertainty, even the ideal controller with access to the true parameters of the system lead to constraint violations. In 8 of these 14 cases, this violation was caused by the initial condition, but the remaining cases resulted in violations further into the growing season. This section provides the results when those outliers are removed, i.e., in the cases where nonlinear model predictive control can theoretically control the system without violations. The results are tabulated in Table 6-3, the average and maximum violations are shown in Figure 6-7 and the costs are in Figure 6-8.

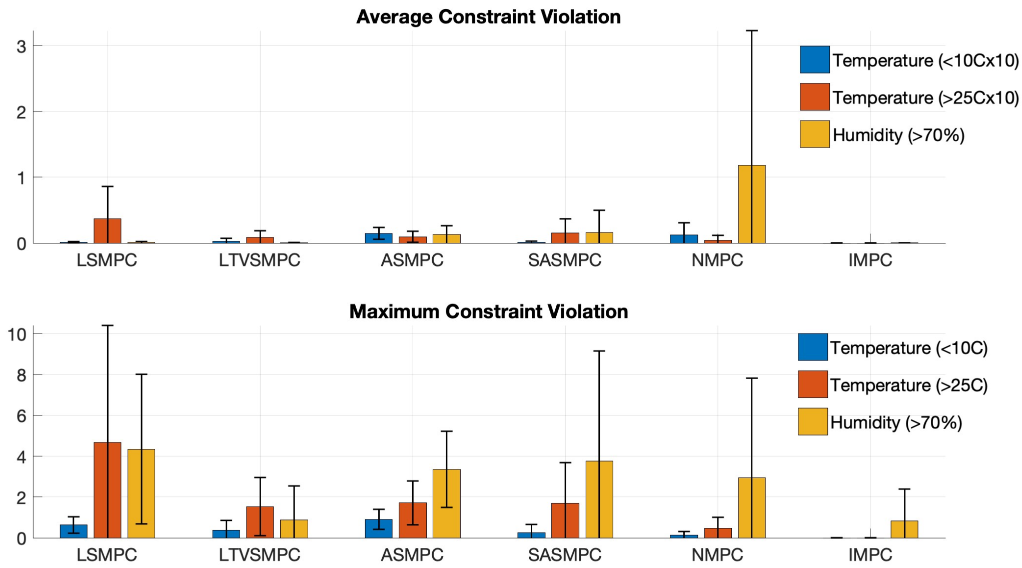

Figure 6-7: Mean and standard deviation of the average constraint violation and maximum constraint violation observed over 24 simulations (6 extreme cases removed) of a 28 day growth period with different parameter realizations, for each controller.

When the extreme cases are removed, the linearized schemes meet their violation rate goals and the adaptive schemes meet their average violation goals. The LTVSMPC still outperforms the LSMPC in terms of constraint compliance, but this time, it also leads to a higher cost. The average costs increased for both schemes when extreme cases were removed. The conservatism of the linearized schemes were betrayed. There are no longer any schemes that led to a profit over the IMPC on average. The only scheme whose costs were reduced by the removal of extreme cases was the ASMPC. It stands out as the scheme with the lowest input costs.

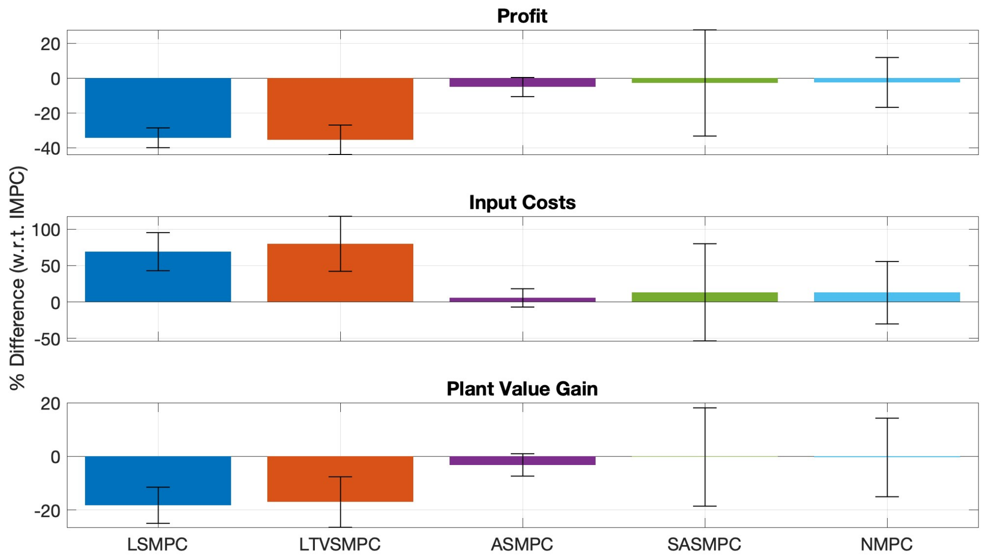

Figure 6-8: Mean and standard deviation of the percentage difference in economic profit, total input costs and the economic value of the increase in plant mass over 24 simulations (6 extreme cases removed) simulations of a 28 day growth period with different parameter realizations, for each controller.

Table 6-3: Controller performance under parameter uncertainty (extreme cases removed).

	LSMPC		**LTVSMPC**		**ASMPC**		**SASMPC**		**NMPC**		**IMPC**	
	μ	σ	μ	σ	μ	σ	μ	σ	μ	σ	μ	σ
Constraint Violations												
Rate (%)	2.083	2.332	1.528	1.649	68.14	36.03	8.830	14.59	42.92	48.09	0.071	0.092
Average ($\times 10^{-1}$)												
Temperature ($< 10^\circ$C)	0.012	0.010	0.025	0.047	0.147	0.090	0.010	0.019	0.119	0.188	0.000	0.000
Temperature ($> 25^\circ$C)	0.366	0.493	0.087	0.100	0.096	0.084	0.152	0.215	0.046	0.075	0.000	0.000
Humidity ($> 70\%$)	0.088	0.134	0.021	0.064	1.287	1.342	1.638	3.341	11.84	20.45	0.008	0.016
Maximum												
Temperature ($< 10^\circ$C)	0.628	0.403	0.366	0.488	0.906	0.491	0.249	0.407	0.137	0.174	0.000	0.000
Temperature ($> 25^\circ$C)	4.685	5.721	1.531	1.425	1.711	1.075	1.704	1.979	0.461	0.544	0.000	0.000
Humidity ($> 70\%$)	4.347	3.665	0.883	1.657	3.355	1.866	3.761	5.392	2.934	4.89	0.834	1.554
Costs Compared to IMPC($\Delta\%$)												
Profit	-34.28	5.672	-35.42	8.437	-5.175	5.479	-2.838	30.44	-2.511	14.29	0.000	0.000
Input Costs	69.10	26.14	79.88	37.72	5.662	12.57	13.30	66.68	12.77	42.81	0.000	0.000
Growth Value	-18.24	6.736	-17.04	9.414	-3.186	4.176	-0.248	18.33	-0.399	14.64	0.000	0.000
Computation Time (s)												
Average	1.080	0.580	1.151	0.599	0.204	0.106	0.221	0.116	0.236	0.122	0.208	0.108
Maximum	3.959	2.225	3.156	1.717	1.218	0.663	2.354	1.562	1.349	0.716	1.043	0.596

6-3 Control Scheme Comparison

In general, the LSMPC leads to more constraint violations and more costs compared to the schemes linearized around a trajectory. The results support the idea that the performance of the linearized controller can be improved by linearizing around a trajectory. A significant factor in the extra cost of the LSMPC is its inability to properly utilize the carbon dioxide input due to the linearization. The difference between the LTVSMPC and the NSMPC is marginal. The only big difference is the increased computational cost of the NSMPC which is not justified by the otherwise negligible improvements in performance.

The SASMPC was constructed to reduce the violations of the ASMPC. The average violations for humidity are plotted in Figure 6-9. Under weather forecast uncertainty, it behaved as planned and reduced the violations slightly at a small increase in cost. However, under parameter uncertainty, it lead to comparable violations and a lower cost with high variance. Although it performs better on average, the fact that its results have a much higher variance indicate that the SASMPC fails in its goal of being a safer form of ASMPC under parametric uncertainty. This failure is rooted in its tendency to stay away from violations, which contradict the nature of the adaptive constraints which require observed constraint violations to properly adapt to disturbances. This can be seen in Figure 6-10. The ASMPC was able to adapt to the parameters in all but 8 of the 30 cases considered. It should be noted again that the corresponding cases resulted in violations even when controlled by an ideal controller. The SASMPC adapts in the beginning but fails in most cases after a period of no violation ends with a series of considerable violations. The violation can accumulate to a point where it would take a period of no violations longer than the entire growth period for the constraints to relax again. Capping the tracker for the average violations is a way to manage this problem, but it was not implemented in this work. The formulation of the adaptive constraints can be further improved by investigating the effect of the choice of decay rate.

What remains is the comparison between the linearized and analytical schemes. The LTVSMPC and the ASMPC are seemingly the best representations of the two approaches. Under weather uncertainty, the observed constraint violations are comparable, but the ASMPC results in a lower cost and even lower input costs. The inputs costs are especially important as even if the expected yield does not materialize, the input costs will. Under parametric uncertainty, the performances of the controllers are more divergent. The LTVSMPC contains conservative assumptions in its formulation which results in a very high cost, especially in the input costs, along with impressive reductions in the constraint violations. The ASMPC is able to mitigate violations to a lesser extent and manages this at an acceptable cost. The ASMPC is also computationally equivalent to the NMPC and does not require any information about the uncertainty to function properly. This makes adaptive schemes more practical to implement. The overall performance of the ASMPC seems preferable to the performance of the LTVSMPC, although there is not enough information to claim that the ASMPC is definitively the better control scheme for the problem at hand, the results strongly support that it is at least a contender and deserves attention.

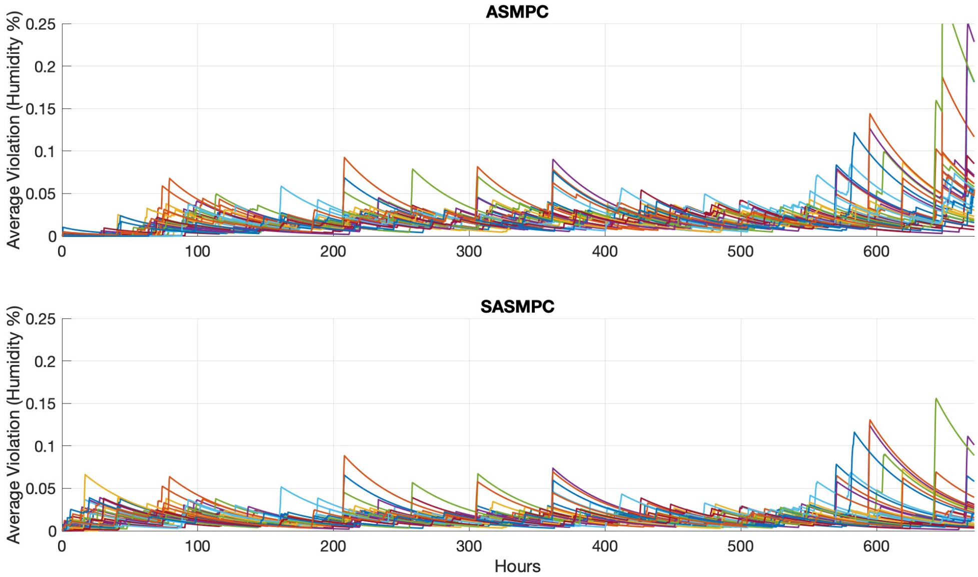

Figure 6-9: Decaying average relative humidity constraint violations under weather forecast uncertainty.

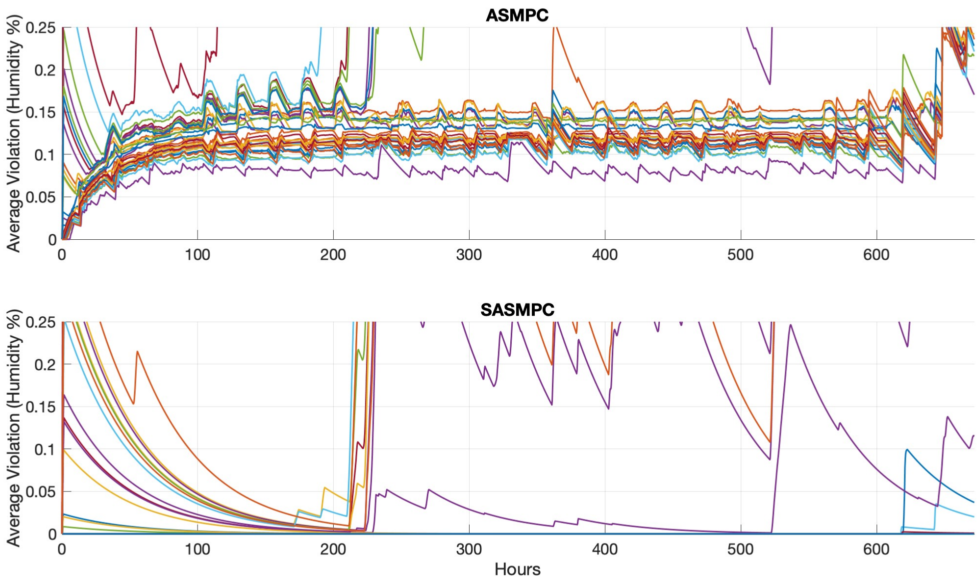

Figure 6-10: Decaying average relative humidity constraint violations under parameter uncertainty.

Chapter 7

Conclusions

Several stochastic model predictive control schemes were formulated for the climate control in a lettuce greenhouse in order to reduce constraint violations under weather or parameter uncertainty. Two distinct approaches were taken in the formulations, system linearization and adaptive average violation constraints. The formulated schemes were tested in simulation alongside deterministic controllers.

Stochastic model predictive control schemes obtained by system linearization were able to successfully impose stochastic constraints of less than 5% of operation spent under violation in simulations, without severely impacting computational requirements. Lower cost and lower maximum constraint violations were observed when the system was linearized around a trajectory instead of a point. Moreover, this was achieved with a minimal additional impact on computational demands. Simply linearizing around a point does not sufficiently represent the impact of the inputs further into the prediction horizon when the weather conditions will have changed. Linearizing a trajectory is shown to be more effective in its representation.

The linearized schemes were quite conservative under parametric uncertainty as the underlying uncertainy was not modelled as Gaussian, which led to conservative assumptions in the formulation through Chebychev's inequality. This resulted in a significant increase in costs. They did not meet the maximum violation rate imposed by the stochastic constraint in simulation under parameter uncertainty. They did however, result in violations which were close to the results of an ideal scheme with access to the correct model parameters, which also resulted in violations above the requirements. The effect of the parameters were not examined in detail, it is possible that some parameter realizations in the simulations, which are not a likely occurrence in reality, lead to a system which has no solution completely within the constraints. Healthier results can be obtained if the parametric uncertainty is modelled more carefully.

The adaptive schemes relying on tracking the average constraint violation were originally proposed for linear systems [31]. In this work, they were adapted for use in a nonlinear system, modified and simplified. The resulting scheme tracks the observed violations and the time and tightens constraints when the observed average violation is above the requirements and relaxes them when its below, leading to reduced conservatism. This tightening is kept constant through the prediction horizon resulting in a computationally equivalent problem to the deterministic case. The scheme does not require prior information on the uncertainty. In simulation, the schemes were able to constrain the average violation rate as intended in general, with exceptions in some extreme parameter uncertainty realizations. The adaptive schemes achieved a lower cost compared to the linearized schemes with comparable violations under weather uncertainty. Under parameter uncertainty, they resulted in more violations, but achieved a significantly lower cost. They were even able to profit over the deterministic controller in some situations by relaxing constraints when the parameter realizations make it harder to violate them.

The results indicate that linearizing around a trajectory can improve the performance of model predictive control schemes for nonlinear systems obtained through system linearization. Stochastic linearized schemes however, may be too conservative and any linearization error may be unnecessary. In applications where small violations can be tolerated and economic optimality is desired, adaptive average constraint violations deserve attention as an easy-to-implement scheme with noteworthy performance. The scheme requires further improvements and investigation into the effect of the decay rate and the dynamics of the uncertainty on its performance. Moreover, it requires further comparison with other methods, such as scenario-based stochastic model predictive control, and trials on other applications to reveal its true utility.

Appendix A

Additional Figures

A-1 Weather Data

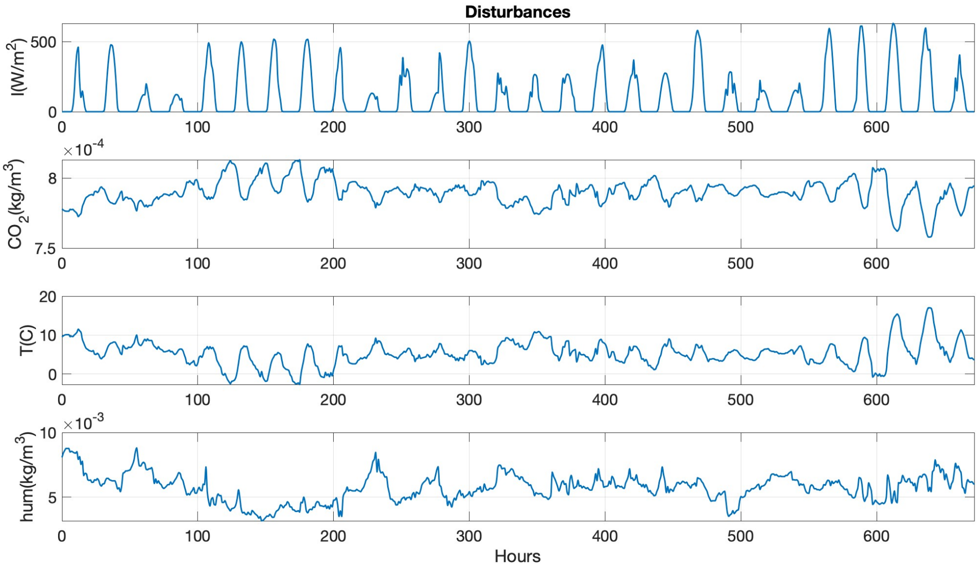

A-2 Weather Forecast Uncertainty

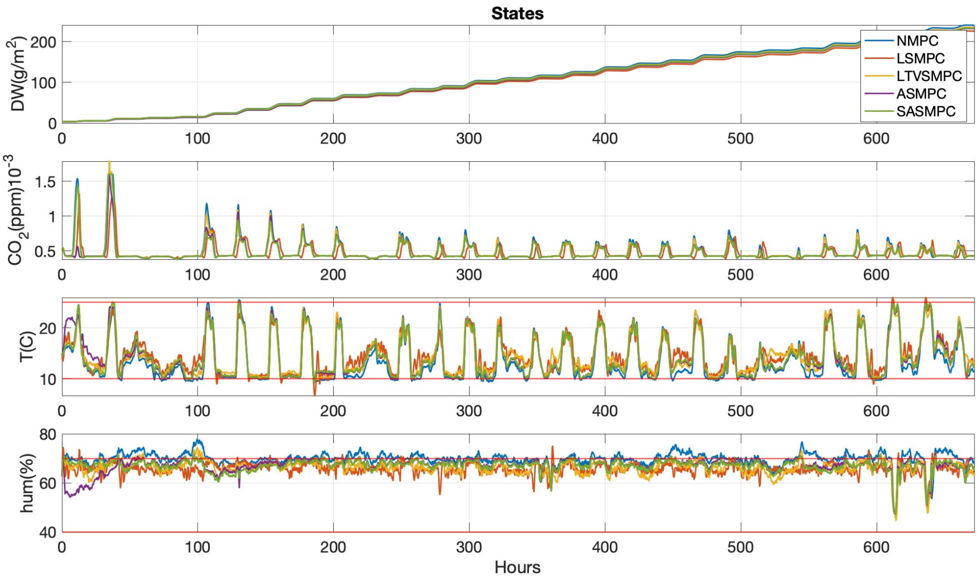

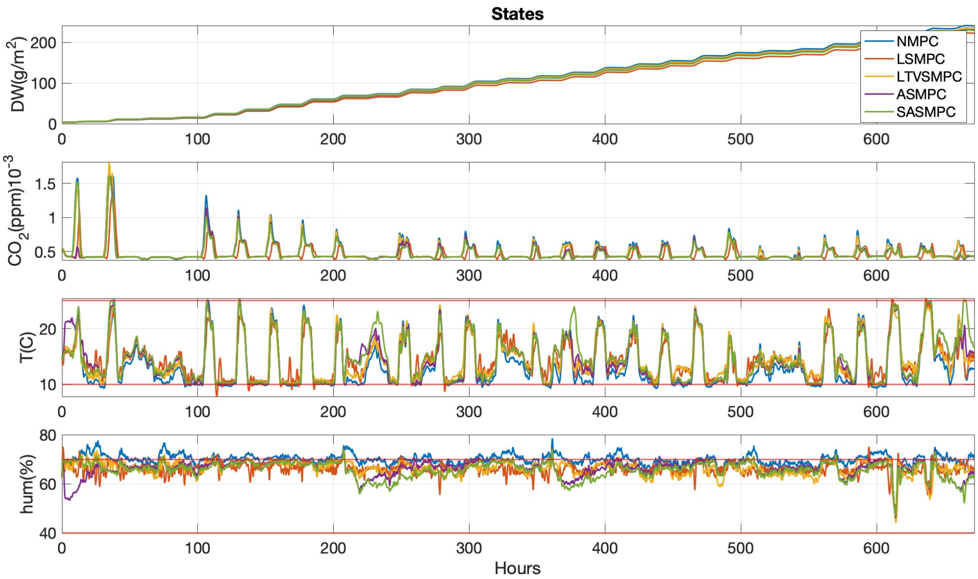

A-3 Parameter Uncertainty

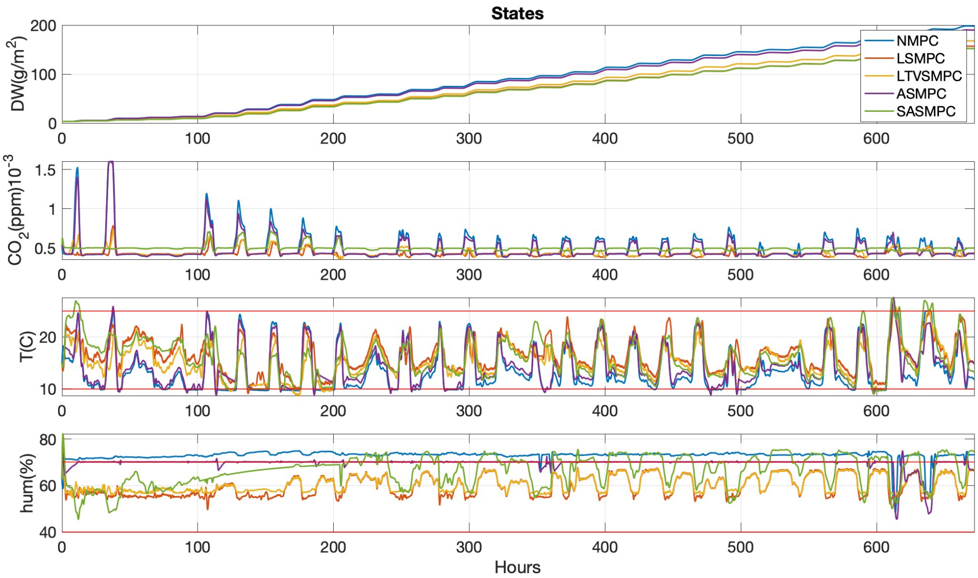

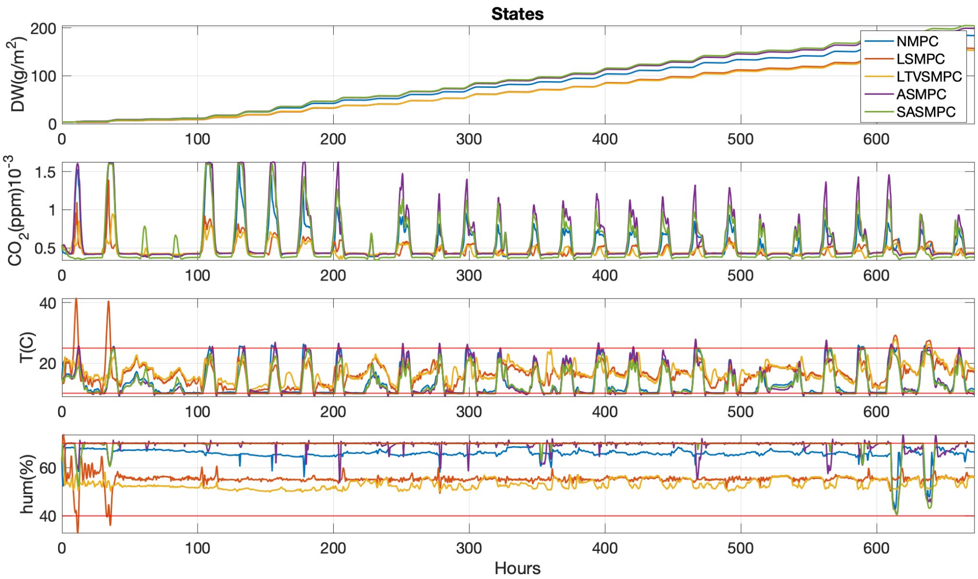

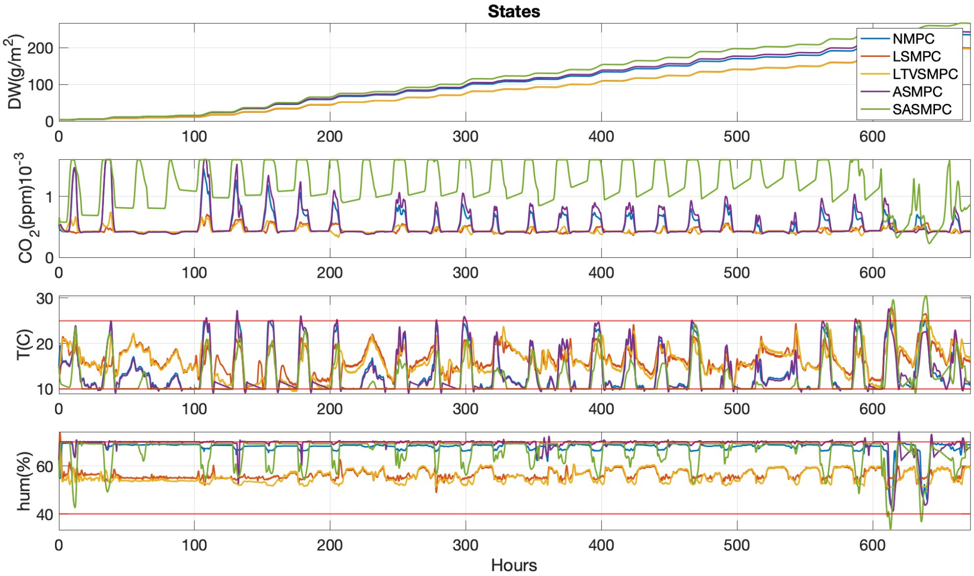
States
DW(g/m^2)
CO$_2$(ppm)10^{-3}
T(C)
hum(%)
Hours
NMPC
LSMPC
LTVSMPC
ASMPC
SASMPC

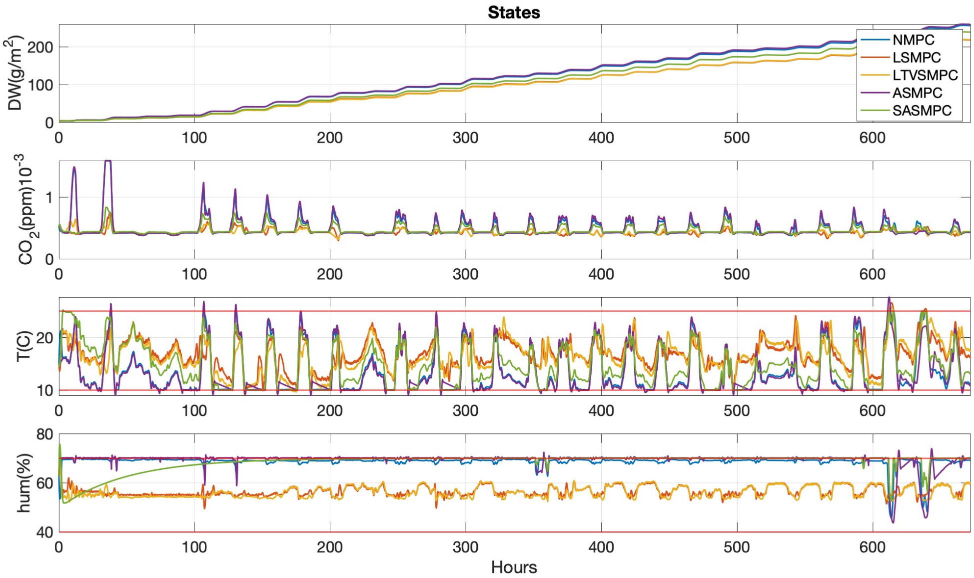
States
DW(g/m^2)
CO$_2$(ppm)10^{-3}
T(C)
hum(%)
Hours
NMPC
LSMPC
LTVSMPC
ASMPC
SASMPC

A-3-1 Extreme Cases

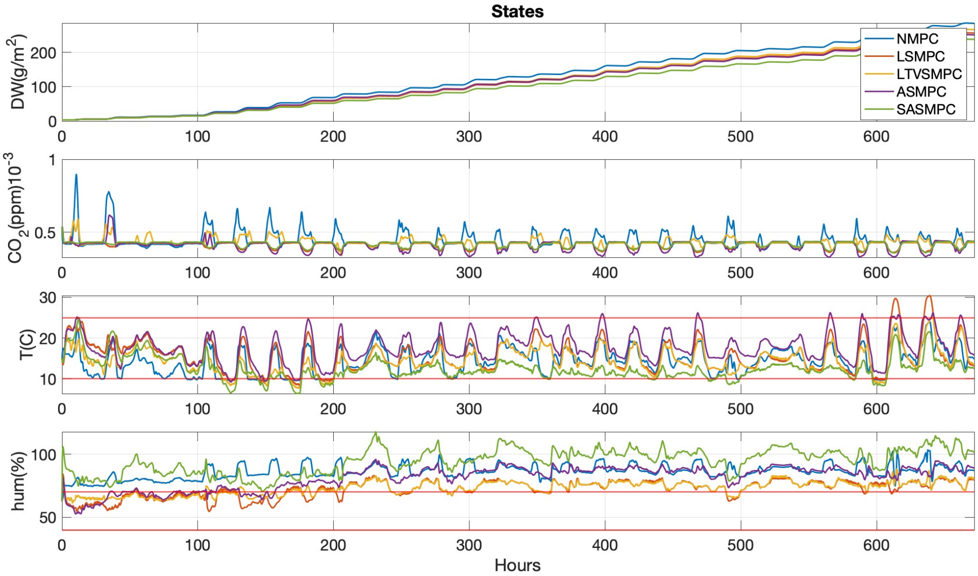

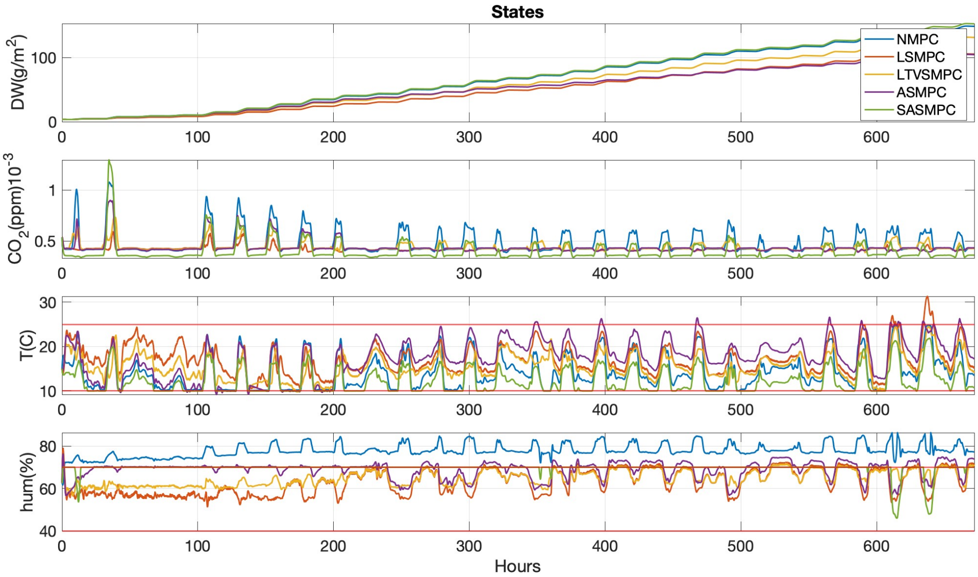

Bibliography

[1] Rishi Amrit, James B Rawlings, and David Angeli. Economic optimization using model predictive control with a terminal cost. *Annual Reviews in Control*, 35(2):178–186, 2011.

[2] Joel AE Andersson, Joris Gillis, Greg Horn, James B Rawlings, and Moritz Diehl. Casadi: a software framework for nonlinear optimization and optimal control. *Mathematical Programming Computation*, 11:1–36, 2019.

[3] Karl Johan Astrom, Karl Henrik Johansson, and Qing-Guo Wang. Design of decoupled pid controllers for mimo systems. In *Proceedings of the 2001 American Control Conference.(Cat. No. 01CH37148)*, volume 3, pages 2015–2020. IEEE, 2001.

[4] José A Aznar-Sánchez, Juan F Velasco-Muñoz, Belén López-Felices, and Isabel M Román-Sánchez. An analysis of global research trends on greenhouse technology: towards a sustainable agriculture. *International journal of environmental research and public health*, 17(2):664, 2020.

[5] Alberto Bemporad and Manfred Morari. Robust model predictive control: A survey. In *Robustness in identification and control*, pages 207–226. Springer, 2007.

[6] Daniele Bernardini and Alberto Bemporad. Scenario-based model predictive control of stochastic constrained linear systems. In *Proceedings of the 48h IEEE Conference on Decision and Control (CDC) held jointly with 2009 28th Chinese Control Conference*, pages 6333–6338. IEEE, 2009.

[7] Daniele Bernardini and Alberto Bemporad. Stabilizing model predictive control of stochastic constrained linear systems. *IEEE Transactions on Automatic Control*, 57(6):1468–1480, 2011.

[8] Xavier Blasco, Miguel Martínez, Juan M Herrero, Cesar Ramos, and Javier Sanchis. Model-based predictive control of greenhouse climate for reducing energy and water consumption. *Computers and electronics in agriculture*, 55(1):49–70, 2007.

[9] Sjoerd Boersma, Congcong Sun, and Simon Van Mourik. Robust sample-based model predictive control of a greenhouse system with parametric uncertainty. *IFAC-PapersOnLine*, 55(32):177–182, 2022.

[10] Gerardus PA Bot. *Greenhouse climate: from physical processes to a dynamic model (Ph.D. thesis)*. Wageningen University and Research, 1983.

[11] Giuseppe Carlo Calafiore and Marco C Campi. The scenario approach to robust control design. *IEEE Transactions on automatic control*, 51(5):742–753, 2006.

[12] Marco C Campi and Simone Garatti. The exact feasibility of randomized solutions of uncertain convex programs. *SIAM Journal on Optimization*, 19(3):1211–1230, 2008.

[13] Peter J Campo and Manfred Morari. Robust model predictive control. In *1987 American control conference*, pages 1021–1026. IEEE, 1987.

[14] Mark Cannon, Basil Kouvaritakis, Saša V Raković, and Qifeng Cheng. Stochastic tubes in model predictive control with probabilistic constraints. *IEEE Transactions on Automatic Control*, 56(1):194–200, 2010.

[15] Wei-Han Chen and Fengqi You. Smart greenhouse control under harsh climate conditions based on data-driven robust model predictive control with principal component analysis and kernel density estimation. *Journal of Process Control*, 107:103–113, 2021.

[16] Luigi Chisci, J Anthony Rossiter, and Giovanni Zappa. Systems with persistent disturbances: predictive control with restricted constraints. *Automatica*, 37(7):1019–1028, 2001.

[17] Stefano Raimondi Cominesi, Marcello Farina, Luca Giulioni, Bruno Picasso, and Riccardo Scattolini. A two-layer stochastic model predictive control scheme for microgrids. *IEEE Transactions on Control Systems Technology*, 26(1):1–13, 2017.

[18] Jeremy Coulson, John Lygeros, and Florian Dörfler. Distributionally robust chance constrained data-enabled predictive control. *IEEE Transactions on Automatic Control*, 67(7):3289–3304, 2021.

[19] Ad NM de Koning. *Development and dry matter distribution in glasshouse tomato: a quantitative approach (Ph.D. thesis)*. Wageningen University and Research, 1994.

[20] MA Eden, RA Hill, Robert Beresford, and A Stewart. The influence of inoculum concentration, relative humidity, and temperature on infection of greenhouse tomatoes by botrytis cinerea. *Plant Pathology*, 45(4):795–806, 1996.

[21] MY El Ghoumari, H-J Tantau, and J Serrano. Non-linear constrained mpc: Real-time implementation of greenhouse air temperature control. *Computers and electronics in agriculture*, 49(3):345–356, 2005.

[22] Matthew Ellis, Helen Durand, and Panagiotis D Christofides. A tutorial review of economic model predictive control methods. *Journal of Process Control*, 24(8):1156–1178, 2014.

[23] Marcello Farina, Luca Giulioni, and Riccardo Scattolini. Stochastic linear model predictive control with chance constraints–a review. *Journal of Process Control*, 44:53–67, 2016.

[24] Paul J Goulart, Eric C Kerrigan, and Jan M Maciejowski. Optimization over state feedback policies for robust control with constraints. *Automatica*, 42(4):523–533, 2006.

[25] Sergio Grammatico, Xiaojing Zhang, Kostas Margellos, Paul Goulart, and John Lygeros. A scenario approach for non-convex control design. *IEEE Transactions on Automatic Control*, 61(2):334–345, 2015.

[26] JK Gruber, JL Guzmán, F Rodríguez, C Bordons, M Berenguel, and JA Sánchez. Nonlinear mpc based on a volterra series model for greenhouse temperature control using natural ventilation. *Control Engineering Practice*, 19(4):354–366, 2011.

[27] Lukas Hewing, Kim P Wabersich, and Melanie N Zeilinger. Recursively feasible stochastic model predictive control using indirect feedback. *Automatica*, 119:109095, 2020.

[28] James W Jones, Ehud Dayan, LH Allen, Herman Van Keulen, and Hugo Challa. A dynamic tomato growth and yield model (tomgro). *Transactions of the ASAE*, 34(2):663–0672, 1991.

[29] FLK Kempkes, J Janse, and S Hemming. Greenhouse concept with high insulating double glass with coatings and new climate control strategies; from design to results from tomato experiments. In *International Symposium on New Technologies for Environment Control, Energy-Saving and Crop Production in Greenhouse and Plant 1037*, pages 83–92, 2013.

[30] B.A. Kimball. Simulation of the energy balance of a greenhouse. *Agricultural Meteorology*, 11:243–260, 1973.

[31] Milan Korda, Ravi Gondhalekar, Frauke Oldewurtel, and Colin N. Jones. Stochastic mpc framework for controlling the average constraint violation. *IEEE Transactions on Automatic Control*, 59(7):1706–1721, 2014.

[32] Basil Kouvaritakis, Mark Cannon, Saša V Raković, and Qifeng Cheng. Explicit use of probabilistic distributions in linear predictive control. *Automatica*, 46(10):1719–1724, 2010.

[33] Wouter JP Kuijpers, Duarte J Antunes, Simon van Mourik, Eldert J van Henten, and Marinus JG van de Molengraft. Weather forecast error modelling and performance analysis of automatic greenhouse climate control. *biosystems engineering*, 214:207–229, 2022.

[34] Tan Liu, Qingyun Yuan, and Yonggang Wang. Hierarchical optimization control based on crop growth model for greenhouse light environment. *Computers and Electronics in Agriculture*, 180:105854, 2021.

[35] Matthias Lorenzen, Fabrizio Dabbene, Roberto Tempo, and Frank Allgöwer. Constraint-tightening and stability in stochastic model predictive control. *IEEE Transactions on Automatic Control*, 62(7):3165–3177, 2016.

[36] Yudong Ma, Jadranko Matuško, and Francesco Borrelli. Stochastic model predictive control for building hvac systems: Complexity and conservatism. *IEEE Transactions on Control Systems Technology*, 23(1):101–116, 2014.

[37] Samuel Mallick, Filippo Airaldi, Azita Dabiri, Congcong Sun, and Bart De Schutter. Reinforcement learning-based model predictive control for greenhouse climate control. *Smart Agricultural Technology*, 10:100751, 2025.

[38] Albert W Marshall and Ingram Olkin. Multivariate chebyshev inequalities. *The Annals of Mathematical Statistics*, pages 1001–1014, 1960.

[39] David Q Mayne. Model predictive control: Recent developments and future promise. *Automatica*, 50(12):2967–2986, 2014.

[40] David Q Mayne, James B Rawlings, Christopher V Rao, and Pierre OM Scokaert. Constrained model predictive control: Stability and optimality. *Automatica*, 36(6):789–814, 2000.

[41] David Q Mayne, María M Seron, and Saša V Raković. Robust model predictive control of constrained linear systems with bounded disturbances. *Automatica*, 41(2):219–224, 2005.

[42] Ali Mesbah. Stochastic model predictive control: An overview and perspectives for future research. *IEEE Control Systems Magazine*, 36(6):30–44, 2016.

[43] Ali Mesbah, Stefan Streif, Rolf Findeisen, and Richard D Braatz. Stochastic nonlinear model predictive control with probabilistic constraints. In *2014 American control conference*, pages 2413–2419. IEEE, 2014.

[44] Manfred Morari and Jay H Lee. Model predictive control: past, present and future. *Computers & chemical engineering*, 23(4-5):667–682, 1999.

[45] Frauke Oldewurtel, Alessandra Parisio, Colin N Jones, Dimitrios Gyalistras, Markus Gwerder, Vanessa Stauch, Beat Lehmann, and Manfred Morari. Use of model predictive control and weather forecasts for energy efficient building climate control. *Energy and buildings*, 45:15–27, 2012.

[46] Frauke Oldewurtel, David Sturzenegger, Peyman Mohajerin Esfahani, Göran Andersson, Manfred Morari, and John Lygeros. Adaptively constrained stochastic model predictive control for closed-loop constraint satisfaction. In *2013 American Control Conference*, pages 4674–4681. IEEE, 2013.

[47] Masahiro Ono and Brian C Williams. Iterative risk allocation: A new approach to robust model predictive control with a joint chance constraint. In *2008 47th IEEE Conference on Decision and Control*, pages 3427–3432. IEEE, 2008.

[48] Alessandra Parisio, Evangelos Rikos, and Luigi Glielmo. Stochastic model predictive control for economic/environmental operation management of microgrids: An experimental case study. *Journal of Process Control*, 43:24–37, 2016.

[49] James A Primbs and Chang Hwan Sung. Stochastic receding horizon control of constrained linear systems with state and control multiplicative noise. *IEEE transactions on Automatic Control*, 54(2):221–230, 2009.

[50] S Joe Qin and Thomas A Badgwell. A survey of industrial model predictive control technology. *Control engineering practice*, 11(7):733–764, 2003.

[51] R Tyrrell Rockafellar, Stanislav Uryasev, et al. Optimization of conditional value-at-risk. *Journal of risk*, 2:21–42, 2000.

[52] J Anthony Rossiter, Basil Kouvaritakis, and MJ Rice. A numerically robust state-space approach to stable-predictive control strategies. *Automatica*, 34(1):65–73, 1998.

[53] Georg Schildbach, Lorenzo Fagiano, Christoph Frei, and Manfred Morari. The scenario approach for stochastic model predictive control with bounds on closed-loop constraint violations. *Automatica*, 50(12):3009–3018, 2014.

[54] Alexander T Schwarm and Michael Nikolaou. Chance-constrained model predictive control. *AIChE Journal*, 45(8):1743–1752, 1999.

[55] M. Kudret Selçuk. Analysis, design, and performance evaluation of controlled-environment greenhouses. In *ASHRAE National Meeting*, page 43, Kansas City, 1970.

[56] Jan Lorenz Svensen, Xiaodong Cheng, Sjoerd Boersma, and Congcong Sun. Chance-constrained stochastic mpc of greenhouse production systems with parametric uncertainty. *Computers and Electronics in Agriculture*, 217:108578, 2024.

[57] DG Sweeney, DW Hand, G Slack, and JHM Thornley. Modelling the growth of winter lettuce. *Mathematics and plant physiology*, 1981.

[58] Tadashi Takakura and Genji Ohara. Direct digital control of plant growth. ii physiological analysis of cucumber plants. *Journal of Agricultural Meteorology*, 32(3):107–115, 1976.

[59] Theodore W Tibbitts and G Bottenberg. Growth of lettuce under controlled humidity levels1. *Journal of the American Society for Horticultural Science*, 101(1):70–73, 1976.

[60] EJ Van Henten. *Greenhouse climate management: an optimal control approach (Ph.D. thesis)*. Wageningen University and Research, 1994.

[61] EJ Van Henten. Validation of a dynamic lettuce growth model for greenhouse climate control. *Agricultural Systems*, 45(1):55–72, 1994.

[62] Dennis Van Hessem and Okko Bosgra. Stochastic closed-loop model predictive control of continuous nonlinear chemical processes. *Journal of Process Control*, 16(3):225–241, 2006.

[63] Bart PG Van Parys, Daniel Kuhn, Paul J Goulart, and Manfred Morari. Distributionally robust control of constrained stochastic systems. *IEEE Transactions on Automatic Control*, 61(2):430–442, 2015.

[64] Gerrit Van Straten, Hugo Challa, and Fokke Buwalda. Towards user accepted optimal control of greenhouse climate. *Computers and electronics in agriculture*, 26(3):221–238, 2000.

[65] Andreas Wächter and Lorenz T Biegler. On the implementation of an interior-point filter line-search algorithm for large-scale nonlinear programming. *Mathematical programming*, 106:25–57, 2006.

[66] Florian Weissel, Marco F Huber, and Uwe D Hanebeck. Stochastic nonlinear model predictive control based on gaussian mixture approximations. In *Informatics in Control, Automation and Robotics: Selected Papers from the International Conference on Informatics in Control, Automation and Robotics 2007*, pages 239–252. Springer, 2009.

[67] Xiaojing Zhang, Sergio Grammatico, Georg Schildbach, Paul Goulart, and John Lygeros. On the sample size of randomized mpc for chance-constrained systems with application to building climate control. In *2014 european control conference (ECC)*, pages 478–483. IEEE, 2014.

[68] Steve Zymler, Daniel Kuhn, and Berç Rustem. Distributionally robust joint chance constraints with second-order moment information. *Mathematical Programming*, 137:167–198, 2013.